CrossMark

ORIGINAL PAPER

Global motion analysis of energy-based control for 3-link planar robot with a single actuator at the first joint

Yannian Liu · Xin Xin

Abstract This paper studies nonlinear control of a 3-link planar robot moving in the vertical plane with only the first joint being actuated while the two other revolute joints are passive (called the APP robot below). A nonlinear energy-based controller is proposed, whose objective is to drive the APP robot into an invariant set where the first link is in the upright position and the total mechanical energy converges to its value at the upright equilibrium point (all three links are in the upright position). By presenting and using a new property of the motion of the APP robot, without any condition on its mechanical parameters, this paper proves that if the control gains are larger than specific lower bounds, then only a measure-zero set of initial conditions converges to three strictly unstable equilibrium points instead of converging to the invariant set. This paper presents numerical results for a physical 3-link planar robot to validate the obtained theoretical results and to demonstrate a switch–and–stabilize maneuver in which the energy-based controller is switched to a linear state feedback controller that stabilizes the APP robot at its upright equilibrium point.

1 Introduction

Studies on underactuated mechanical systems, which possess fewer actuators than degrees of freedom (DOF), have received considerable interest in the last two decades. In mobile robotic locomotion (legged, wheeled, swimming, flying, etc.), underactuation is an inherent property of the system since the degrees of freedom that describe net body motion are not directly actuated. Moreover, underactuation may alternatively be a consequence of on-purpose "minimalistic" design without using full actuation or that of the failure of one or more actuators. However, it is difficult to control these systems due to their complex nonlinear dynamics and nonholonomic behavior, see pioneer works in [10,15,25,26], and other interesting results in [2–4,7–9,13,18,19,22,24,27–29].

Many researchers investigated the notion of energy shaping in controlling underactuated mechanical systems since energy is an important variable related to the motion of the systems. For an underactuated mechanical system with generalized coordinate $\theta(t)$, [10] and

Y. Liu
Graduate School of Natural Science and Technology, Okayama University, 1-1-1 Tsushima-naka, Okayama 700-8530, Japan
e-mail: ynliujp@yahoo.co.jp

X. Xin (✉)
Faculty of Computer Science and Systems Engineering, Okayama Prefectural University, 111 Kuboki, Soja, Okayama 719-1197, Japan
e-mail: xxin@cse.oka-pu.ac.jp

[15] addressed the simultaneous control of both its total mechanical energy $E(\boldsymbol{\theta}(t), \dot{\boldsymbol{\theta}}(t))$ and actuated variable(s) $\boldsymbol{\theta}_a(t)$; that is, whether one can design a controller to achieve

$$\lim_{t \to \infty} E(\boldsymbol{\theta}(t), \dot{\boldsymbol{\theta}}(t)) = E_r, \tag{1}$$

$$\lim_{t \to \infty} \boldsymbol{\theta}_a(t) = \boldsymbol{\theta}_{ar}, \quad \lim_{t \to \infty} \dot{\boldsymbol{\theta}}_a(t) = \mathbf{0}, \tag{2}$$

where E_r is a given constant, $\boldsymbol{\theta}_{ar}$ is a given constant vector, and $\mathbf{0}$ is zero column vector with a compatible size.

For the Pendubot [11,15], and the Acrobot [32], objectives (1) and (2) have been shown to be achievable for the swing-up and stabilizing control problem, which is to drive the robot to a small neighborhood of its UEP (upright equilibrium point) and then stabilize it around that point, where all links are in the upright position. The above energy-based control is applied to stabilize an unstable equilibrium point of the butterfly robot in [6]. However, [31] showed that objectives (1) and (2) cannot be achieved simultaneously for the swing-up and stabilizing control problem of a 2-link underactuated robot with a particular counterweight connected to the passive first joint. For a set-point control for a folded configuration of 3-link gymnastic planar robot with the first joint being passive (unactuated) and the second and third joints being active (actuated), we proved in [17] that objectives (1) and (2) can be achieved simultaneously if the mechanical parameters of the robot satisfy certain conditions, and we show via a numerical example that objectives (1) and (2) are not achieved simultaneously when the mechanical parameters of the robot do not satisfy these conditions. Thus, for an underactuated system with particular mechanical parameters, although objective (2) can be achieved for example by the partial feedback linearization in [26], it is not clear whether objectives (1) and (2) can be achieved simultaneously.

Although there are many results for mechanical systems with underactuation degree one [1,10,12], that is, the number of control inputs is one less than that of degrees of freedom, designing and analyzing controllers for mechanical systems with underactuation degree greater than one are still a challenging problem. For the double pendulum in a cart, [30] showed that objectives (1) and (2) can be achieved with E_r being the highest potential energy of the double pendulum for almost all initial conditions of the system. Building

on this previous research, for a 3-link planar robot in a vertical plane with its first joint being active and the rest joints being passive, this paper studies a theoretically challenging problem, that is, whether objectives (1) and (2) corresponding to the UEP (all three links are in the upright position), and objective (3)

$$\lim_{t \to \infty} \boldsymbol{\theta}(t) = \mathbf{0}_3, \quad \lim_{t \to \infty} \dot{\boldsymbol{\theta}}(t) = \mathbf{0}_3, \tag{3}$$

are achievable for almost every initial condition, where $\boldsymbol{\theta}(t)$ is the vector of three link angles of the robot, and $\mathbf{0}_3$ denotes a zero column vector with size 3. This is the ultimate objective of stabilizing the robot at the UEP. We call this robot APP (Active Passive Passive) robot below.

This paper applies the procedure in [10,15] to derive an energy-based controller for the APP robot. By presenting and using a new property of the motion of the APP robot, without any condition on its mechanical parameters, this paper proves that if the control gains are larger than specific lower bounds, then objectives (1) and (2) corresponding to the UEP are achievable for all initial conditions with the exception of a set of Lebesgue measure zero.

Indeed, first, the new property is that if link 1 of the APP robot does not move under a constant torque on joint 1, then links 2 and 3 do not move. To the best of our knowledge, this property has not yet been proved. We present a strict proof of this property for any mechanical parameters of the APP robot, any constant angle of joint 1, and corresponding constant torque by using some properties of the mechanical parameters of the APP robot. Second, the measure-zero set of initial conditions converges to three strictly unstable equilibrium points: the up–up–down, up–down–up, and up–down–down equilibrium points, where, for example, up–up–down means that links 1, 2, and 3 are in the upright, upright, and downward positions, respectively.

The presented control law achieves objectives (1) and (2) corresponding to the UEP for almost all initial conditions but does not achieve objective (3), since the UEP becomes strictly unstable. This motivates the use of the additional LQR-based linear state feedback law. It is worth pointing out that the linear controller succeeds in achieving only local stabilization, from initial conditions in a close neighborhood of the UEP. The combination of switching between the two control laws is then shown to practically achieve all objectives (1), (2), and (3), but no formal proof is found yet that shows that this ALWAYS works.
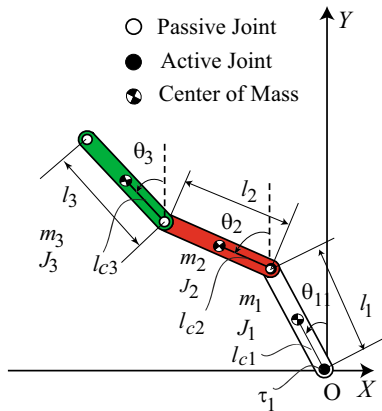
Fig. 1 APP robot: 3-link planar robot with a single actuator at the first joint

The remainder of the paper is organized as follows: Sect. 2 gives some preliminary knowledge and problem formulation. Section 3 presents the main results of this paper. Section 4 makes some discussions. Section 5 gives numerical simulation results for a physical 3-link planar robot in [20]. Section 6 makes some concluding remarks. Certain proofs whose details are not central to the flow of the paper are gathered in the appendices. For brevity, we omit time argument t in the expression of a variable if it is clear from the context.

2 Preliminary knowledge and problem formulation

2.1 Preliminary knowledge

Consider a 3-link planar robot with a single actuator at joint 1 (at the origin) shown in Fig. 1. For link i ($i = 1, 2, 3$), m_i is its mass, l_i is its length, l_{ci} is the distance from joint i to its center of mass (COM), and J_i is the moment of inertia around its COM, τ_1 is the torque acting at joint 1, and θ_i is the angle measured counterclockwise from the positive Y-axis. In this paper, θ_1, the angle of active joint 1, is dealt in $\mathbb{R}$; θ_2 and θ_3, the angles of the passive links, are dealt with in $\mathbb{S}^2$ (a torus) and take value in $(-\pi, \pi]$.

The motion equation of the APP robot is

$$M(\boldsymbol{\theta})\ddot{\boldsymbol{\theta}} + C(\boldsymbol{\theta}, \dot{\boldsymbol{\theta}})\dot{\boldsymbol{\theta}} + g(\boldsymbol{\theta}) = b\tau_1, \qquad (4)$$

where $\boldsymbol{\theta} = \begin{bmatrix} \theta_1, \theta_2, \theta_3 \end{bmatrix}^{\mathrm{T}}$ and

$$M(\boldsymbol{\theta})$$
$$= \begin{bmatrix} \alpha_{11} & \alpha_{12}\cos(\theta_2 - \theta_1) & \alpha_{13}\cos(\theta_3 - \theta_1) \\ \alpha_{12}\cos(\theta_2 - \theta_1) & \alpha_{22} & \alpha_{23}\cos(\theta_3 - \theta_2) \\ \alpha_{13}\cos(\theta_3 - \theta_1) & \alpha_{23}\cos(\theta_3 - \theta_2) & \alpha_{33} \end{bmatrix}, \qquad (5)$$

$$C(\boldsymbol{\theta}, \dot{\boldsymbol{\theta}})$$
$$= \begin{bmatrix} 0 & -\alpha_{12}\dot{\theta}_2\sin(\theta_2 - \theta_1) & -\alpha_{13}\dot{\theta}_3\sin(\theta_3 - \theta_1) \\ \alpha_{12}\dot{\theta}_1\sin(\theta_2 - \theta_1) & 0 & -\alpha_{23}\dot{\theta}_3\sin(\theta_3 - \theta_2) \\ \alpha_{13}\dot{\theta}_1\sin(\theta_3 - \theta_1) & \alpha_{23}\dot{\theta}_2\sin(\theta_3 - \theta_2) & 0 \end{bmatrix}, \qquad (6)$$

$$g(\boldsymbol{\theta}) = \begin{bmatrix} -\beta_1\sin\theta_1 \\ -\beta_2\sin\theta_2 \\ -\beta_3\sin\theta_3 \end{bmatrix}, \quad b = \begin{bmatrix} 1 \\ 0 \\ 0 \end{bmatrix} \qquad (7)$$

with

$$\begin{cases} \alpha_{11} = J_1 + m_1 l_{c1}^2 + (m_2 + m_3)l_1^2, \\ \alpha_{22} = J_2 + m_2 l_{c2}^2 + m_3 l_2^2, \\ \alpha_{33} = J_3 + m_3 l_{c3}^2, \\ \alpha_{12} = (m_2 l_{c2} + m_3 l_2)l_1, \\ \alpha_{13} = m_3 l_1 l_{c3}, \\ \alpha_{23} = m_3 l_2 l_{c3}, \\ \beta_1 = (m_1 l_{c1} + m_2 l_1 + m_3 l_1)g, \\ \beta_2 = (m_2 l_{c2} + m_3 l_2)g, \\ \beta_3 = m_3 l_{c3}g, \end{cases} \qquad (8)$$

where g is the acceleration of gravity.

The total mechanical energy of the APP robot is

$$E(\boldsymbol{\theta}, \dot{\boldsymbol{\theta}}) = \frac{1}{2}\dot{\boldsymbol{\theta}}^{\mathrm{T}}M(\boldsymbol{\theta})\dot{\boldsymbol{\theta}} + P(\boldsymbol{\theta}), \qquad (9)$$

where $P(\boldsymbol{\theta})$ is its potential energy defined by

$$P(\boldsymbol{\theta}) = \beta_1\cos\theta_1 + \beta_2\cos\theta_2 + \beta_3\cos\theta_3. \qquad (10)$$

From (4), we have

$$\begin{aligned} \dot{E}(\boldsymbol{\theta}, \dot{\boldsymbol{\theta}}) &= \dot{\boldsymbol{\theta}}^{\mathrm{T}}M(\boldsymbol{\theta})\ddot{\boldsymbol{\theta}} + \frac{1}{2}\dot{\boldsymbol{\theta}}^{\mathrm{T}}\dot{M}(\boldsymbol{\theta})\dot{\boldsymbol{\theta}} + \dot{\boldsymbol{\theta}}^{\mathrm{T}}g(\boldsymbol{\theta}) \\ &= \dot{\boldsymbol{\theta}}^{\mathrm{T}}\left(-C(\boldsymbol{\theta}, \dot{\boldsymbol{\theta}})\dot{\boldsymbol{\theta}} - g(\boldsymbol{\theta}) + b\tau_1\right) \\ &\quad + \frac{1}{2}\dot{\boldsymbol{\theta}}^{\mathrm{T}}\dot{M}(\boldsymbol{\theta})\dot{\boldsymbol{\theta}} + \dot{\boldsymbol{\theta}}^{\mathrm{T}}g(\boldsymbol{\theta}) \\ &= \dot{\boldsymbol{\theta}}^{\mathrm{T}}b\tau_1 + \frac{1}{2}\dot{\boldsymbol{\theta}}^{\mathrm{T}}(\dot{M}(\boldsymbol{\theta}) - 2C(\boldsymbol{\theta}, \dot{\boldsymbol{\theta}}))\dot{\boldsymbol{\theta}} \qquad (11) \\ &= \dot{\theta}_1\tau_1, \qquad (12) \end{aligned}$$

where the second term in the right-hand side of (11) is 0 since $\dot{M}(\boldsymbol{\theta}) - 2C(\boldsymbol{\theta}, \dot{\boldsymbol{\theta}})$ is a skew-symmetric matrix which can be verified directly by using (5) and (6).

2.2 Problem formulation

Consider the following UEP:

$$\boldsymbol{\theta}(t) = \mathbf{0}_3, \quad \dot{\boldsymbol{\theta}}(t) = \mathbf{0}_3. \tag{13}$$

For $E(\boldsymbol{\theta}, \dot{\boldsymbol{\theta}})$, θ_1, and $\dot{\theta}_1$, we design and analyze a controller to address whether objectives (1) and (2) can be achieved, where E_r is the highest potential energy of the APP robot expressed as:

$$E_r = E(\boldsymbol{\theta}(t), \dot{\boldsymbol{\theta}}(t)) \Big|_{\boldsymbol{\theta}(t)=\mathbf{0}_3, \ \dot{\boldsymbol{\theta}}(t)=\mathbf{0}_3} = \beta_1 + \beta_2 + \beta_3, \tag{14}$$

$\boldsymbol{\theta}_a(t) = \theta_1(t)$, and $\boldsymbol{\theta}_{ar} = 0$.

3 Main results

Define the following controller:

$$\tau_1(t)$$
$$= \frac{k_D B^{\mathrm{T}} M^{-1}(\boldsymbol{\theta}(t))(C(\boldsymbol{\theta}(t), \dot{\boldsymbol{\theta}}(t))\dot{\boldsymbol{\theta}}(t) + g(\boldsymbol{\theta}(t))) - k_V \dot{\theta}_1(t) - k_P \theta_1(t)}{\eta(\boldsymbol{\theta}(t), \dot{\boldsymbol{\theta}}(t))}, \tag{15}$$

where

$$\eta(\boldsymbol{\theta}(t), \dot{\boldsymbol{\theta}}(t)) = E(\boldsymbol{\theta}(t), \dot{\boldsymbol{\theta}}(t)) - E_r + k_D b^{\mathrm{T}} M^{-1}(\boldsymbol{\theta}(t)) b. \tag{16}$$

Below we present the following five lemmas and one theorem. Lemma 1 is about a condition on gain k_D to guarantee that controller (15) is well defined, whose proof is given in "Appendix 1."

Lemma 1 $\eta(\boldsymbol{\theta}(t), \dot{\boldsymbol{\theta}}(t))$ in (16) is positive for any $(\boldsymbol{\theta}(t), \dot{\boldsymbol{\theta}}(t))$ if and only if k_D satisfies

$$k_D > k_{Dm}$$
$$= \max_{\substack{-\pi \ \le \theta_i(t) \le \pi \\ i = 1, 2, 3}} \left((E_r - P(\boldsymbol{\theta}(t))) \left(b^{\mathrm{T}} M^{-1}(\boldsymbol{\theta}(t)) b \right)^{-1} \right). \tag{17}$$

Lemma 2 is about the invariant set to which every solution of the closed-loop system converges, whose proof is given in "Appendix 2."

Lemma 2 *Consider the closed-loop system consisting of APP robot (4) and controller (15). If k_D satisfies (17), and*

$$k_V > 0, \tag{18}$$
$$k_P > 0, \tag{19}$$

then the closed-loop solution, $(\boldsymbol{\theta}(t), \dot{\boldsymbol{\theta}}(t))$, converges to the following invariant set:

$$W = \left\{ (\boldsymbol{\theta}(t), \dot{\boldsymbol{\theta}}(t)) \ \Big| \ \frac{1}{2}\alpha_{22}\dot{\theta}_2^2(t) + \alpha_{23}\dot{\theta}_2(t)\dot{\theta}_3(t) \right.$$
$$\times \cos(\theta_3(t) - \theta_2(t)) + \frac{1}{2}\alpha_{33}\dot{\theta}_3^2(t)$$
$$\left. + P(\boldsymbol{\theta}(t)) \equiv E^*, \quad \theta_1(t) \equiv \theta_1^* \right\}, \tag{20}$$

where "$\equiv$" denotes the equation holds for all t.

Lemma 3 shows a new property of the motion of the APP robot with its proof in "Appendix 3."

Lemma 3 *Consider APP robot (4). Suppose $\theta_1(t) \equiv \theta_1^*$ and $\tau_1(t) \equiv \tau_1^*$ with θ_1^* and τ_1^* being constants; that is, link 1 does not move under a constant torque on joint 1. Then, links 2 and 3 do not move; that is,*

$$\dot{\theta}_2(t) \equiv 0, \quad \dot{\theta}_3(t) \equiv 0 \tag{21}$$

for any mechanical parameters described in (8) for the APP robot, θ_1^*, and τ_1^*.

Lemma 4 characterizes the invariant set the W in (20) further under a condition on gain k_P, whose proof is presented in "Appendix 4."

Lemma 4 *Consider the closed-loop system consisting of APP robot (4) and controller (15). Suppose that k_D satisfies (17), k_V satisfies (18), and k_P satisfies*

$$k_P > k_{Pm} = \max_{\pi \le w \le 2\pi}$$
$$\times \frac{-\beta_1 \left(\beta_1(1 - \cos w) + 2\beta_2 + 2\beta_3\right)\sin w}{w}. \tag{22}$$

Then, the invariant set W in (20) becomes the union

$$W = W_r \cup \Omega_s, \tag{23}$$

where

$$W_r = \left\{ (\boldsymbol{\theta}(t), \dot{\boldsymbol{\theta}}(t)) \ \Big| \ \frac{1}{2}\alpha_{22}\dot{\theta}_2^2(t) \right.$$
$$+ \alpha_{23}\dot{\theta}_2(t)\dot{\theta}_3(t)\cos(\theta_3(t) - \theta_2(t)) + \frac{1}{2}\alpha_{33}\dot{\theta}_3^2(t)$$
$$+ \beta_2(\cos\theta_2(t) - 1) + \beta_3(\cos\theta_3(t) - 1) = 0,$$
$$\left. \theta_1(t) \equiv 0 \right\} \tag{24}$$

and

$$\Omega_s = \left\{ (\boldsymbol{\theta}^*, \mathbf{0}_3) \mid \boldsymbol{\theta}^* \equiv \begin{bmatrix} 0, & 0, & \pi \end{bmatrix}^T, \begin{bmatrix} 0, & \pi, & 0 \end{bmatrix}^T, \right.$$
$$\left. \times \begin{bmatrix} 0, & \pi, & \pi \end{bmatrix}^T \right\}. \tag{25}$$

Moreover, the UEP is the only equilibrium point in W_r.

Lemma 5 is about the stability of all equilibrium points of the closed-loop system, whose proof is presented in "Appendix 5."

Lemma 5 *Consider the closed-loop system consisting of APP robot (4) and controller (15). Given the bounds on the gains in (17), (18), and (22). The UEP and the equilibrium points in Ω_s are all strictly unstable.*

We present the following main result of this paper.

Theorem 1 *Consider the closed-loop system consisting of APP robot (4) and controller (15). Given the bounds on the gains in (17), (18), and (22). The closed-loop solution, $(\boldsymbol{\theta}(t), \dot{\boldsymbol{\theta}}(t))$, converges to the invariant set W_r in (24), except for the measure-zero set of initial conditions that converge to the strictly unstable equilibrium points in the Ω_s in (25). The UEP is the only equilibrium point in W_r and is strictly unstable. Controller (15) achieves objectives (1) and (2) corresponding to the UEP for almost all initial conditions but does not achieve objective (3).*

Proof From Lemmas 4 and 5, since each equilibrium point of Ω_s is strictly unstable; that is, the Jacobian matrix evaluated at each equilibrium point of Ω_s has at least one eigenvalue in the open right-half plane, the set of initial conditions from which the closed-loop solution converges to Ω_s is of Lebesgue measure zero, see, e.g., [21] (p. 1225). In other words, from all initial conditions with the exception of a set of Lebesgue measure zero, the closed-loop solution $(\boldsymbol{\theta}(t), \dot{\boldsymbol{\theta}}(t))$ converges to the invariant set W_r. Thus, controller (15) achieves objectives (1) and (2) corresponding to the UEP for almost all initial conditions. From Lemmas 4 and 5, we know that the UEP is the only equilibrium point in W_r and is strictly unstable. Therefore, controller (15) does not achieve objective (3). □

4 Discussion

4.1 On the invariant set W_r

Theorem 1 shows that objectives (1) and (2) corresponding to the UEP are achieved for almost all initial conditions under the proposed energy-based controller (15), provided that the conditions on control gains are satisfied. Even though the UEP is contained in the invariant set W_r in (24) in $t \in (0, \infty)$, it is unclear that the solution trajectories will come into a close neighborhood of the UEP. In this sense, this paper does not give a general algorithm to guarantee theoretically for achieving the true practical objective of the APP control: stabilization of the UEP from almost any initial conditions.

From our simulation results for the APP robot with mechanical parameters in [20], under the proposed controller (15) there existed moments in $t \in (0, \infty)$ when the robot came into a close neighborhood of the UEP for several initial conditions we simulated. Please refer two examples in Sects. 5.1 and 5.2. The combination of switching between the two control laws is shown by simulation to practically achieve all objectives (1), (2), and (3), but no formal proof is found yet that shows that this ALWAYS works. We would like to investigate it further in the future.

4.2 On Lemma 3 and its proof

There are various applications of symbolic computation in robot manipulator design and analysis, for example, in kinematics, dynamics, trajectory planning, and control [23]. This paper also shows an application of symbolic computation in the proof of Lemma 3, which is important for proving Theorem 1. Below we discuss Lemma 3 and its proof.

First, Lemma 3 means that for APP robot (4), if link 1 is at rest under a constant torque on joint 1, then the entire system is in an equilibrium point. Lemma 3 seems to be intuitive: As long as links 2 and 3 move, the forces acting at the distal joint of link 1 (joint 2) will change which results in a varying moment at the proximal joint of link 1 (joint 1); thus, a varying torque must be applied at joint 1 to keep link 1 balanced. However, by analyzing all the forces acting at three joints, we cannot find more information than motion equation (4). The details are omitted.

Second, it is very difficult to prove Lemma 3 for *any mechanical parameters described in (8) for the APP robot, any constant angle of joint 1, and corresponding constant torque* because of the strong nonlinear coupling of two passive joints of the APP robot when link 1 of the robot is at rest under a constant

torque. Indeed, in its proof we used the properties of the mechanical parameters shown in Lemmas 6 and 7. If $\sin\theta_1^* = 0$ (link 1 at the vertical position), then the proof of Lemma 3 can be simplified considerably (without need to use symbolic computation), please refer the result for the double pendulum in a cart in [30]. However, if $\sin\theta_1^* \neq 0$ (link 1 not at the vertical position), then the proof is much more involved as shown in "Appendix 3."

If the mechanical parameters of links 2 and 3 of the robot satisfy $a^2 - ab - ae + 1 \neq 0$, where a, b, and e are defined in (34), then we do not need the analysis of Case 2 ($a^2 - ab - ae + 1 = 0$) in the proof of Lemma 3 which is complicated and involved, please refer "Eq. 37 of Appendix 3." Note that the physical 3-link robot in [20] which is used in the simulation in Sect. 5 satisfies $a^2 - ab - ae + 1 \neq 0$. Moreover, when link 2 of a 3-link robot has a massless rod with a point mass at its end; that is, $l_{c2} = l_2$ and $J_2 = 0$, then from (8) we obtain

$$a = \frac{\beta_2}{\beta_3} = \frac{(m_2 + m_3)l_2}{m_3 l_{c3}}, \quad b = \frac{\alpha_{22}}{\alpha_{23}} = \frac{(m_2 + m_3)l_2}{m_3 l_{c3}}.$$

Thus, $a = b$; together with $ae > 1$ due to Lemma 6, $a^2 - ab - ae + 1 < 0$. Note that the massless rod assumption is often used in pendulum-type systems, see, e.g., [5].

5 Simulation results

We present numerical simulation results for an APP robot with its mechanical parameters being given in Table 1, which are taken from the physical 3-link planar robot in [20]. We took $g = 9.8$ m/s^2.

From Theorem 1, under controller (15) with conditions (17) and (22); that is, $k_D > 11.2100$ J^2 s^2 and $k_P > 81.1069$ J^2 for this APP robot, and with condi-

Table 1 Mechanical parameters of the physical 3-link planar robot in [20]

	Link 1	Link 2	Link 3
m_i (kg)	0.41	4.10	0.41
l_i (m)	0.268	0.258	0.268
l_{ci} (m)	0.134	0.128	0.095
J_i (kg m^2)	4.52×10^{-3}	6.11×10^{-2}	4.52×10^{-3}

tion $k_V > 0$, objectives (1) and (2) corresponding to the UEP are achievable from all initial conditions with the exception of a set of Lebesgue measure zero.

Since the UEP is strictly unstable under the proposed energy-based controller according to Lemma 5, when the APP robot is swung up close to the UEP, to stabilize it around the UEP, we need to switch the energy-based controller to a local stabilizing controller designed by LQR method. Define $\boldsymbol{x}(t) = \left[\theta_1(t), \theta_2(t), \theta_3(t), \dot{\theta}_1(t), \dot{\theta}_2(t), \dot{\theta}_3(t)\right]^{\mathrm{T}}$. The LQR controller is

$$\tau_1(t) = -\boldsymbol{K}\boldsymbol{x}(t), \tag{26}$$

where

$$\boldsymbol{K} = \left[\, 24.8073, \ -125.5004, \ 276.3903, \ 10.9221, \ 5.2260, \ 39.4850 \,\right],$$

which was obtained by using the MATLAB function "lqr" for which the weight related to the torque was chosen to be 1, and the weight matrix related to state $\boldsymbol{x}(t)$ was chosen to be a diagonal matrix of 6×6 with the diagonal elements from $(1, 1)$ to $(6, 6)$ being 1, 1, 1, 0.1, 0.1, and 0.1.

The condition for switching controller (15) to controller (26) was set as

$$\begin{aligned} d(t) &= |\theta_1(t)| + |\theta_2(t)| + |\theta_3(t)| \\ &\quad + 0.1|\dot{\theta}_1(t)| + 0.1|\dot{\theta}_2(t)| + 0.1|\dot{\theta}_3(t)| < \epsilon_0 \end{aligned} \tag{27}$$

for given $\epsilon_0 > 0$. Indeed, small ϵ_0 is good for achieving a successful switch from controller (15) to controller (26). On the other hand, big ϵ_0 is good for achieving a quick switch from controller (15) to controller (26). In this paper, we chosen $\epsilon_0 = 0.5$ in (27) by trial and error to achieve a successful and quick switch from controller (15) to controller (26).

Since links 2 and 3 may have rotated several times when the LQR controller is switched, $\theta_i(t)$ $(i = 2, 3)$ may take value out of $(-\pi, \pi)$. Therefore, $\theta_2(t)$ and $\theta_3(t)$ in (26) and (27) are used under modulo operation with divisor 2π and take values in $(-\pi, \pi)$. Note that controller (15) needs more knowledge of the system's parameters and more computation time than controller (26).

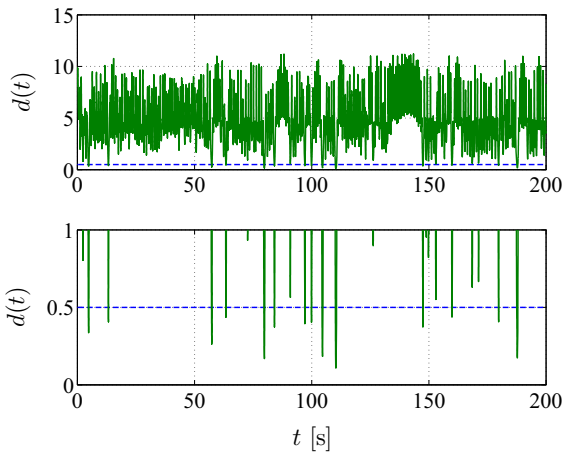Below, we report our simulation results for two initial conditions.

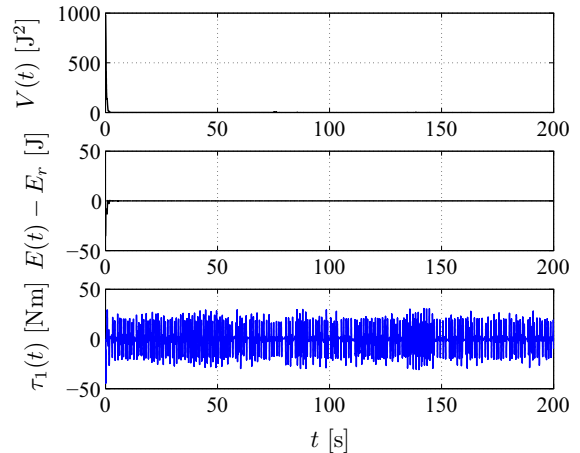**Fig. 2** Time responses of $d(t)$ in (27) under controller (15) with initial condition (28)

Fig. 3 Time responses of $V(t)$, $E(t) - E_r$, and $\tau_1(t)$ under controller (15) with initial condition (28)

5.1 Initial condition 1

We took an initial condition

$$
\begin{aligned}
&\left(\theta_1(0), \theta_2(0), \theta_3(0), \dot{\theta}_1(0), \dot{\theta}_2(0), \dot{\theta}_3(0)\right) \\
&= \left(\frac{5\pi}{6}, \frac{6\pi}{7}, \frac{7\pi}{8}, 0, 0, 0\right),
\end{aligned} \tag{28}
$$

which is close to the downward equilibrium point

$$
\begin{aligned}
&\left(\theta_1(t), \theta_2(t), \theta_3(t), \dot{\theta}_1(t), \dot{\theta}_2(t), \dot{\theta}_3(t)\right) \\
&= (\pi, \pi, \pi, 0, 0, 0).
\end{aligned}
$$

To swing the APP robot up quickly close to the UEP, we took $k_D = 12.8495 \, \mathrm{J}^2 \, \mathrm{s}^2$, $k_P = 101.6513 \, \mathrm{J}^2$, and $k_V = 34.9863 \, \mathrm{J}^2 \mathrm{s}$. Under controller (15), we present the simulation results for $t \in [0, 200]$ s to show whether the switching condition in (27) is satisfied. The simulation results under the energy-based controller (15) are shown in Figs. 2, 3 and 4. From Fig. 2, there were many moments when (27) was satisfied.

Figure 3 shows that $V(t)$ and $E(t) - E_r$ converged to 0 and $\tau_1(t)$ was not constant. Figure 4 shows that $\theta_1(t)$ converged to 0, and $\theta_2(t)$ and $\theta_3(t)$ were time varying. Though $\theta_2(t)$ and $\theta_3(t)$ are treated in $\mathbb{S}^2$, plots of $\theta_2(t)$ and $\theta_3(t)$ in Fig. 4 were not plotted modulo 2π to avoid confusing artificial points of apparent discontinuity. From Figs. 3 and 4, we validated that objectives (1) and (2) corresponding to the UEP were achieved.

In Fig. 3, the control torque $\tau_1(t)$ satisfied -44.4371 Nm $\leq \tau_1(t) \leq 30.5831$ Nm. To see whether these values are small or large, we compare those with the
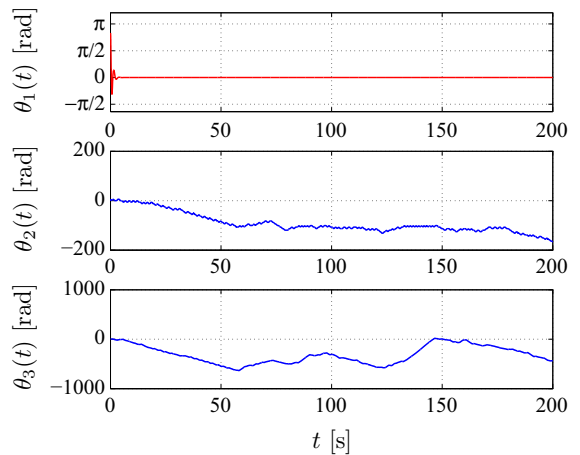

Fig. 4 Time responses of $\theta_1(t)$, $\theta_2(t)$, and $\theta_3(t)$ under controller (15) with initial condition (28)

torque where link 1 is horizontal while the two other links are upward vertical. In such a position, we have $\tau_1(t) = -\beta_1 = -12.3835$ Nm.

When switching condition (27) was satisfied, we switched controller (15) to controller (26). From Fig. 5, the switch was taken at $t = 4.67$ s. Note that the final convergence of $\theta_3(t)$ is -6.2832 rad $= -2\pi$ rad which is 0 rad under modulo operation with divisor 2π. From Fig. 6, we found that the swing-up control and stabilizing control of the APP robot in Table 1 were achieved under controllers (15) and (26).

The simulation result under control (26) for $t \in [0, 0.2]$ s is depicted in Fig. 7, which indicates that controller (26) did not stabilize the APP robot to the
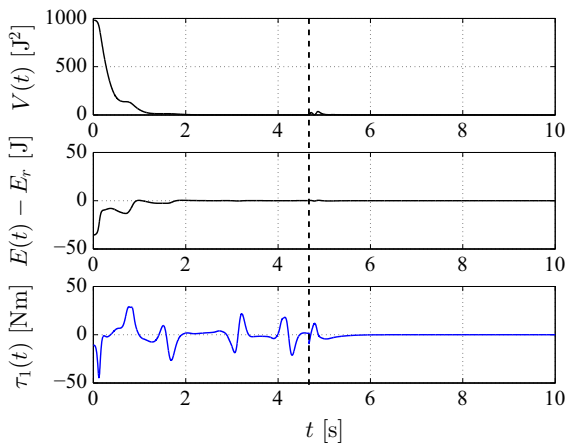
Fig. 5 Time responses of $V(t)$, $E(t) - E_r$, and $\tau_1(t)$ under controllers (15) and (26) with initial condition (28), where the *dashed vertical line* indicates the switching time
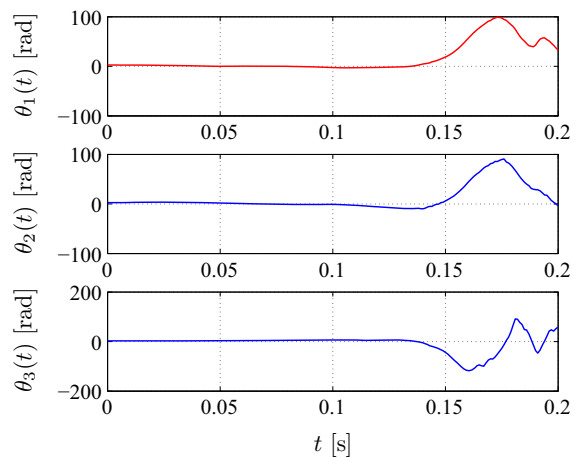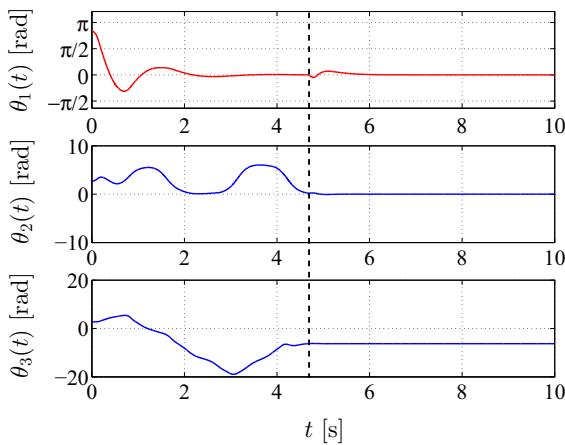

Fig. 6 Time responses of $\theta_1(t)$, $\theta_2(t)$, and $\theta_3(t)$ under controllers (15) and (26) with initial condition (28), where the *dashed vertical line* indicates the switching time

Fig. 7 Time responses of $\theta_1(t)$, $\theta_2(t)$, and $\theta_3(t)$ under controller (26) with initial condition (28)
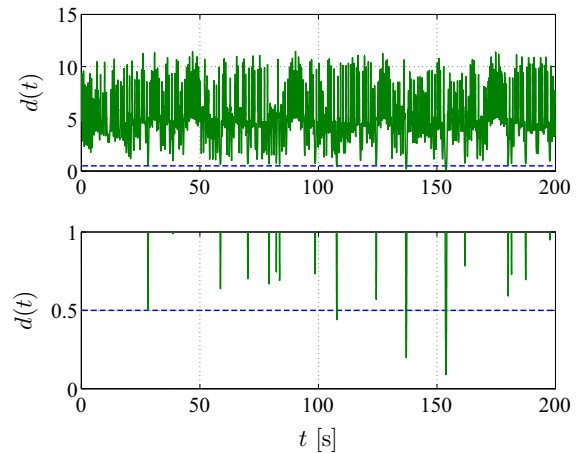

Fig. 8 Time responses of $d(t)$ in (27) with initial condition (29) under controller (15)

UEP from initial condition (28). The maximal value of $\tau_1(t)$ in $t \in [0, 0.2]$ s was 1.0283×10^6 Nm. This shows that to stabilize the APP robot to the UEP from initial condition (28), the proposed controllers (15) and (26) are better than controller (26) only.

5.2 Initial condition 2

We took an initial condition

$$
\begin{aligned}
&\big(\theta_1(0), \theta_2(0), \theta_3(0), \dot{\theta}_1(0), \dot{\theta}_2(0), \dot{\theta}_3(0)\big) \\
&\quad = \Big(\frac{\pi}{2}, \frac{\pi}{2}, \frac{\pi}{2}, 0, 0, 0\Big),
\end{aligned} \tag{29}
$$

where all links are at a stretched horizontal position.

The simulation results under the energy-based controller (15) are shown in Figs. 8, 9 and 10. From Fig. 8, we can see that there were several moments when (27) was satisfied. Figure 9 shows that $V(t)$ and $E(t) - E_r$ converged to 0 and $\tau_1(t)$ was not constant. In Fig. 9, the control torque $\tau_1(t)$ satisfied -32.7102 Nm $\leq \tau_1(t) \leq 30.2021$ Nm. Figure 10 shows that $\theta_1(t)$ converged to 0, and $\theta_2(t)$ and $\theta_3(t)$ were time varying. From Figs. 9 and 10, we validated that objectives (1) and (2) corresponding to the UEP were achieved.

When switching condition (27) was satisfied, we switched controller (15) to controller (26). From Fig. 11, the switch was taken at $t = 107.70$ s. From
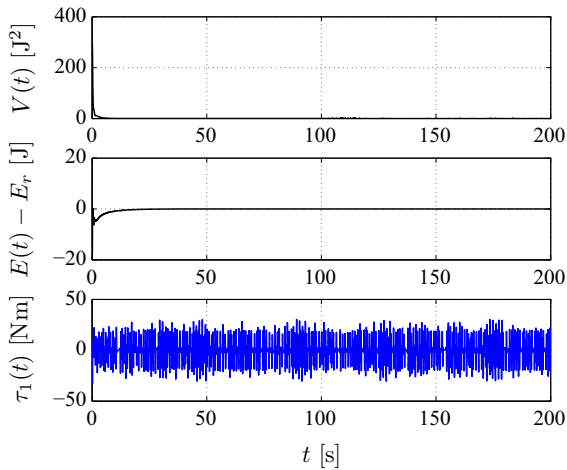
Fig. 9 Time responses of $V(t)$, $E(t) - E_r$, and $\tau_1(t)$ under controller (15) with initial condition (29)
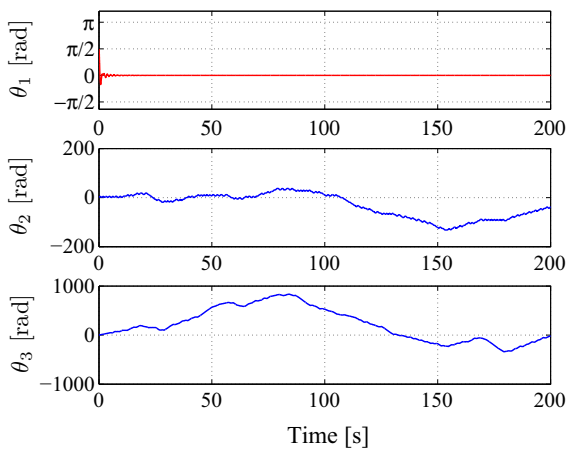

Fig. 10 Time responses of $\theta_1(t)$, $\theta_2(t)$, and $\theta_3(t)$ under controller (15) with initial condition (29)
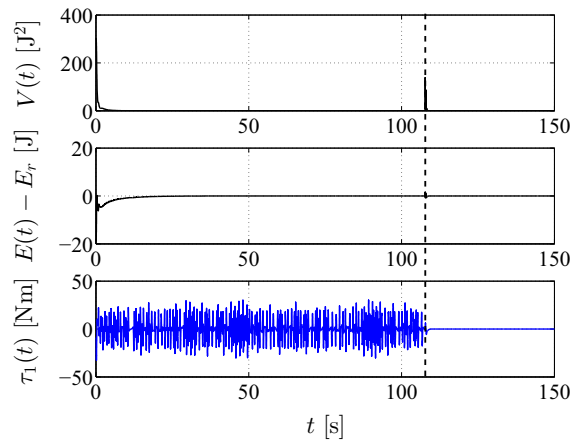

Fig. 11 Time responses of $V(t)$, $E(t) - E_r$, and $\tau_1(t)$ under controllers (15) and (26) with initial condition (29), where the *dashed vertical line* indicates the switching time
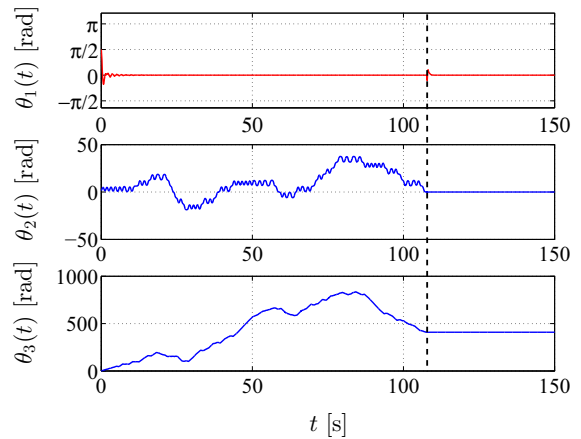

Fig. 12 Time responses of $\theta_1(t)$, $\theta_2(t)$, and $\theta_3(t)$ under controllers (15) and (26) with initial condition (29), where the *dashed vertical line* indicates the switching time

Fig. 12, we found that the swing-up control and stabilizing control of the APP robot in Table 1 were achieved under controllers (15) and (26). We also provide Figs. 13 and 14 only for a short period of the time after switching to the LQR law (26), which will enable zooming into the scale for more effectively displaying the final convergence. Note that the final convergence of $\theta_3(t)$ is 408.4070 rad $= 2\pi \times 65$ rad which is 0 rad under modulo operation with divisor 2π.

The simulation result under controller (26) for $t \in [0,\ 0.2]$ s is depicted in Fig. 15, which indicates that controller (26) did not stabilize the APP robot to the UEP from initial condition (29). The maximal value of $\tau_1(t)$ in $t \in [0,\ 0.2]$ s was 9.0179×10^5 Nm. It can

be seen that the linear control law (26) achieves only local stabilization of the UEP from initial conditions in the close neighborhood of the UEP. Only the combination of both control laws (15) and (26) with the switching rule (27) practically achieves almost global stabilization.

6 Conclusion

For a 3-link planar robot with only the first joint being active (the APP robot), we presented a nonlinear energy-based controller whose objective is to drive the APP robot into an invariant set where the first link is
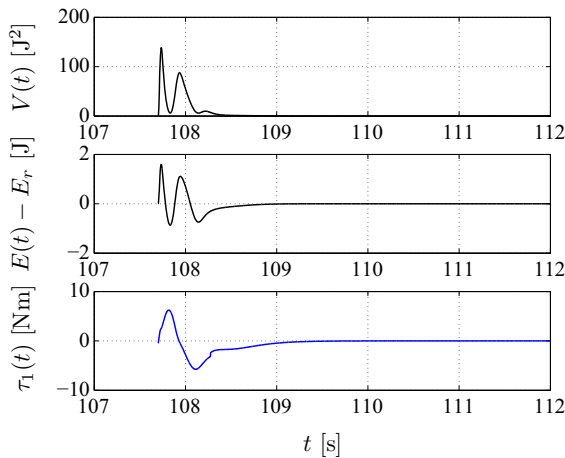
Fig. 13 Time responses of $V(t)$, $E(t) - E_r$, and $\tau_1(t)$ under controllers (15) and (26) with initial condition (29) after the switching at $t = 107.701$ s
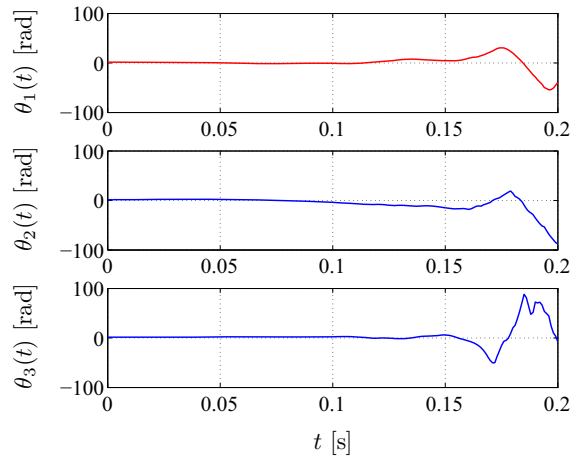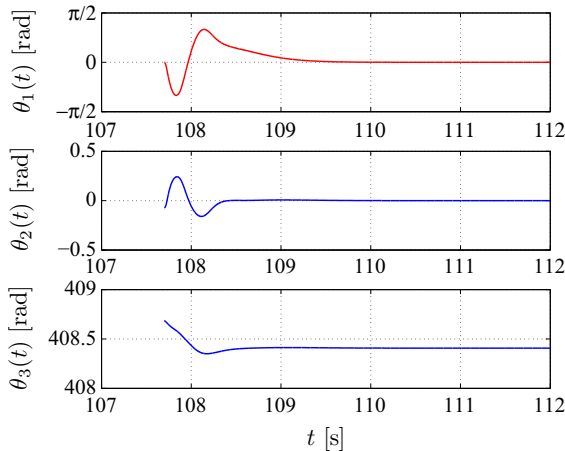

Fig. 14 Time responses of $\theta_1(t)$, $\theta_2(t)$, and $\theta_3(t)$ under controllers (15) and (26) with initial condition (29) after the switching at $t = 107.701$ s

Fig. 15 Time responses of $\theta_1(t)$, $\theta_2(t)$, and $\theta_3(t)$ under controller (26) with initial condition (29)

in the upright position and the total mechanical energy converges to its value at the UEP. By presenting and using a new property of the motion of the APP robot, without any condition on the mechanical parameters of the robot, we proved that if the control gains are larger than specific lower bounds, then only a measure-zero set of initial conditions converges to three strictly unstable equilibrium points instead of converging to the invariant set W_r in (24). The new property described in Lemma 3 is that if link 1 of the APP robot does not move under a constant torque on joint 1, then links 2 and 3 do not move. Three strictly unstable equilib-

rium points are the up–up–down, up–down–up, and up–down–down equilibrium points of the APP robot. The presented energy-based control law achieves objectives (1) and (2) corresponding to the UEP for almost all initial conditions but does not achieve objective (3), since the UEP becomes strictly unstable. We presented numerical results for the physical 3-link planar robot in [20] to validate the obtained theoretical results and to show a successful application to the swing-up and stabilizing control of the APP robot.

Even though the UEP is contained in the invariant set W_r in (24), we are unable to formally prove that the solution is ALWAYS guaranteed to come into a small neighborhood of the UEP at some time. Nevertheless, simulations under physically realistic parameter values show that this is indeed satisfied in practical scenarios.

Appendix 1: Proof of Lemma 1

Using $E(\boldsymbol{\theta}(t), \dot{\boldsymbol{\theta}}(t)) \geq P(\boldsymbol{\theta}(t))$ and $\eta(\boldsymbol{\theta}(t), \dot{\boldsymbol{\theta}}(t))$ in (16), we obtain $\eta(\boldsymbol{\theta}(t), \dot{\boldsymbol{\theta}}(t)) \geq P(\boldsymbol{\theta}(t)) - E_r + k_D \boldsymbol{b}^{\mathrm{T}} \boldsymbol{M}^{-1}(\boldsymbol{\theta}(t))\boldsymbol{b}$. Thus, if (17) holds, then $\eta(\boldsymbol{\theta}(t), \dot{\boldsymbol{\theta}}(t)) > 0$.

To show that (17) is also necessary such that $\eta(\boldsymbol{\theta}(t), \dot{\boldsymbol{\theta}}(t)) > 0$, for any given k_D satisfying $0 <$

$k_D \le k_{Dm}$, we just need to show that there exists an initial condition $(\boldsymbol{\theta}(0), \dot{\boldsymbol{\theta}}(0))$ at which $\eta(\boldsymbol{\theta}(0), \dot{\boldsymbol{\theta}}(0)) = 0$. Indeed, letting $\boldsymbol{\zeta} \in \mathbb{R}^3$ be a value of $\boldsymbol{\theta}(t)$ with $-\pi \le \theta_i(t) \le \pi$ $(i = 1, 2, 3)$ that maximizes the function in the right-hand side of (17); that is, $k_{Dm} = (E_r - P(\boldsymbol{\zeta}))(\boldsymbol{b}^{\mathrm{T}} \boldsymbol{M}^{-1}(\boldsymbol{\zeta}) \boldsymbol{b})^{-1}$.

Choosing $\boldsymbol{\zeta}_d \in \mathbb{R}^3$ such that

$$\frac{1}{2} \boldsymbol{\zeta}_d^{\mathrm{T}} \boldsymbol{M}(\boldsymbol{\zeta}) \boldsymbol{\zeta}_d = (k_{Dm} - k_D) \boldsymbol{b}^{\mathrm{T}} \boldsymbol{M}^{-1}(\boldsymbol{\zeta}) \boldsymbol{b} \ge 0,$$

we obtain

$$\eta(\boldsymbol{\zeta}, \boldsymbol{\zeta}_d) = E(\boldsymbol{\zeta}, \boldsymbol{\zeta}_d) - E_r + k_D \boldsymbol{b}^{\mathrm{T}} \boldsymbol{M}^{-1}(\boldsymbol{\zeta}) \boldsymbol{b} = 0.$$

Thus, $\eta(\boldsymbol{\theta}(t), \dot{\boldsymbol{\theta}}(t)) > 0$ for any $(\boldsymbol{\theta}(t), \dot{\boldsymbol{\theta}}(t))$ if and only if (17) holds. □

Appendix 2: Proof of Lemma 2

First, take the following Lyapunov function candidate:

$$\begin{aligned} V(t) = &\frac{1}{2} (E(\boldsymbol{\theta}(t), \dot{\boldsymbol{\theta}}(t)) - E_r)^2 \\ &+ \frac{k_D}{2} \dot{\theta}_1^2(t) + \frac{k_P}{2} \theta_1^2(t), \end{aligned} \quad (30)$$

where scalars $k_D > 0$ and $k_P > 0$ are control gains. Using (12), we obtain the time derivative of V along the trajectories of (4) as follows:

$$\begin{aligned} \dot{V}(t) = &\dot{\theta}_1(t) \big((E(\boldsymbol{\theta}(t), \dot{\boldsymbol{\theta}}(t)) - E_r) \tau_1(t) \\ &+ k_D \ddot{\theta}_1(t) + k_P \theta_1(t) \big). \end{aligned} \quad (31)$$

Under the control law of $\tau_1(t)$ defined in (15) which is well defined for all initial conditions when k_D satisfies (17) (see Lemma 1), by obtaining $\ddot{\theta}_1(t)$ from (4), we can show that the following relation holds

$$\begin{aligned} &(E(\boldsymbol{\theta}(t), \dot{\boldsymbol{\theta}}(t)) - E_r) \tau_1(t) + k_D \ddot{\theta}_1(t) + k_P \theta_1(t) \\ &= -k_V \dot{\theta}_1(t), \end{aligned} \quad (32)$$

which implies

$$\dot{V}(t) = -k_V \dot{\theta}_1^2(t) \le 0. \quad (33)$$

Second, from $\dot{V}(t) \le 0$ in (33), it follows that $V(t)$ is monotonically nonincreasing and is thus bounded. Using LaSalle's invariance principle [14] shows that the solution of the closed-loop system consisting of (4) and (15) converges to the largest invariant set W where $\dot{V}(t) \equiv 0$; that is, $\dot{\theta}_1(t) \equiv 0$ holds. Thus, $V(t)$ and $\theta_1(t)$ are constants inside the invariant set W. From $V(t)$ in (30), $E(t)$ is also a constant inside the invariant set W. By denoting the constants corresponding to $\theta_1(t)$ and $E(t)$ as θ_1^* and E^*, respectively, and putting $E(t) \equiv E^*$ and $\theta_1(t) \equiv \theta_1^*$ into (9), we show that W is expressed as in (20).

Appendix 3: Proof of Lemma 3

To start with, we provide two lemmas for proving Lemma 3 in "Eq. 34 of Appendix 3." Then, we present two steps of the proof of Lemma 3 in "Eq.35 of Appendix 3" and describe the details of two steps in "Eq.36 of Appendix 3" and "Eq. 37 of Appendix 3." Some algebraic manipulations are carried out with the aid of Mathematica. Please see Sect. 4.2 for the discussion about this proof.

Two preliminary results

Io order to prove Lemma 3, we provide two preliminary results below. Define

$$a = \frac{\beta_2}{\beta_3}, \ \ b = \frac{\alpha_{22}}{\alpha_{23}}, \ \ d = \frac{\beta_3}{\alpha_{23}}, \ \ e = \frac{\alpha_{33}}{\alpha_{23}}, \quad (34)$$

which are determined by the mechanical parameters of links 2 and 3 of the APP robot. We recall a property of the mechanical parameters of a 2-link planar robot presented in Lemma 1 of [32] for links 2 and 3 of the APP robot.

Lemma 6 *For the parameters in* (34)*, the following statements hold:*

$$a \ge b > 0, \quad (35)$$
$$ae > 1. \quad (36)$$

Note that $m_i l_i l_{ci} \ge J_i + m_i l_{ci}^2$ is shown for $i = 1$ in [32] which is critical for showing (35). Equation (36) can be shown by using (8) directly. Using Lemma 6, we obtain the following lemma.

Lemma 7 *If*

$$e = \frac{1 + a^2 - ab}{a}, \quad (37)$$

then

$$a \ne 1, \ \ a > b. \quad (38)$$

Proof If $a = 1$, from (37), we have $b + e = 2$. From (34), we have $b + e \ge 2\sqrt{be} = 2\sqrt{\alpha_{22}\alpha_{33}/\alpha_{23}^2} > 2$, where $\alpha_{22}\alpha_{33} > \alpha_{23}^2$ can be shown by using (8). This raises a contradiction. Thus, $a \ne 1$. If $a = b$, then from (37), $ae = 1$ which contradicts (36). Thus, from (35), we have $a > b$. □

Two steps

Using $\theta_1(t) \equiv \theta_1^*$ and (12), we obtain $\dot{E}(t) = 0$. Thus, $E(t)$ is a constant, which is denoted as E^*. Define the following coordinate transformation:

$$\phi_2(t) = \theta_2(t) - \theta_1^*, \quad \phi_3(t) = \theta_3(t) - \theta_1^*, \quad (39)$$

we prove (21) by the following two steps.

Step 1 Obtain a holonomic constraint of the angle of link 2 described by the following polynomial equation:

$$L = \sum_{i=0}^{N} \xi_i \sin^i \phi_2(t) = 0, \quad \text{for } \forall t, \quad (40)$$

in terms of $\sin \phi_2(t)$, where N is a positive integer to be determined and ξ_i ($i = 0, 1, \ldots, N$) are functions of the mechanical parameters in (8), any possible θ_1^* and E^*.

Step 2 By contradiction, we assume $\dot{\phi}_2(t) = \dot{\theta}_2(t) \not\equiv 0$. Since differentiable function $\phi_2(t)$ is not constant, the polynomial equation in (40) in terms of $\sin \phi_2(t)$ has infinite number of solutions which shows

$$\xi_i = 0, \quad i = 0, 1, \ldots, N. \quad (41)$$

Otherwise, if there exists at least one i ($0 \le i \le N$) such that $\xi_i \ne 0$, then (40) has finite number of solutions. We prove that (41) does not hold for any mechanical parameters described in (8), any possible θ_1^* and E^*. Thus, $\dot{\phi}_2(t) = \dot{\theta}_2(t) \equiv 0$. Moreover, we prove $\dot{\phi}_3(t) = \dot{\theta}_3(t) \equiv 0$.

We present the details of two steps in the following two subsections. For brevity, the time argument t of a variable is omitted below.

Details of Step 1

We carry out Step 1 further by the following substeps.

Step 1.1 Integrate the dynamics of (4) related to joint 1 with $\theta_1 \equiv \theta_1^*$ and $\tau_1 \equiv \tau_1^*$ to obtain

$$a\dot{\phi}_2 \cos \phi_2 + \dot{\phi}_3 \cos \phi_3 = 0, \quad (42)$$

$$a \sin \phi_2 + \sin \phi_3 = \lambda, \quad (43)$$

where λ is a constant. Moreover, if $\sin \theta_1^* = 0$, then $\lambda = 0$.

Step 1.2 Eliminate $\ddot{\phi}_2$ and $\ddot{\phi}_3$ from (4) to obtain

$$F_2 \dot{\phi}_2^2 + F_3 \dot{\phi}_3^2 + F_1 = 0, \quad (44)$$

where F_i ($i = 1, 2, 3$) are functions of $\sin \phi_2$, $\cos \phi_2$, and $\cos \phi_3$. Moreover, obtain the following equation using $E = E^*$ with (39) and (43):

$$\frac{b}{2}\dot{\phi}_2^2 + \dot{\phi}_2\dot{\phi}_3 \cos(\phi_3 - \phi_2)$$
$$+ \frac{e}{2}\dot{\phi}_3^2 + (a \cos \phi_2 + \cos \phi_3)d \cos \theta_1^* = \gamma, \quad (45)$$

where γ is a constant defined by

$$\gamma = \frac{E^* - \beta_1 \cos \theta_1^*}{\alpha_{23}} + \lambda d \sin \theta_1^*. \quad (46)$$

Step 1.3 Eliminate $\dot{\phi}_2$ and $\dot{\phi}_3$ from (42), (44), and (45) to obtain

$$Q_1 + Q_2 \cos \phi_3 = 0, \quad (47)$$

where Q_i ($i = 1, 2$) are functions of $\sin \phi_2$ and $\cos \phi_2$.

Step 1.4 Eliminate $\cos \phi_3$ from (47) by using (43) to obtain

$$Q_1^2 - Q_2^2(1 - \sin^2 \phi_3) = R_1 + R_2 \cos \phi_2 = 0, \quad (48)$$

where R_1 and R_2 are polynomials of $\sin \phi_2$ with the highest orders of 14 and 13, respectively. If $\cos \theta_1^* = 0$, then $R_2 = 0$, and we obtain (40) as:

$$L = R_1 = 0, \quad \text{with } N = 14. \quad (49)$$

If $\cos \theta_1^* \ne 0$, deleting $\cos \phi_2$ from (48) yields that (40), we obtain a polynomial equation of $\sin \phi_2$, as:

$$L = R_1^2 - R_2^2(1 - \sin^2 \phi_2) = 0, \quad \text{with } N = 28. \quad (50)$$

Regarding Step 1.1, using $a = \beta_2/\beta_3 = \alpha_{12}/\alpha_{13}$ due to (8) and using (4) with $\theta_1 \equiv \theta_1^*$, $\tau_1 \equiv \tau_1^*$, and (39), we obtain

$$a\ddot{\phi}_2 \cos \phi_2 + \ddot{\phi}_3 \cos \phi_3 - a\dot{\phi}_2^2 \sin \phi_2 - \dot{\phi}_3^2 \sin \phi_3$$
$$= \frac{\tau_1^* + \beta_1 \sin \theta_1^*}{\alpha_{13}}, \quad (51)$$

$$b\ddot{\phi}_2 + \ddot{\phi}_3 \cos(\phi_3 - \phi_2) - \dot{\phi}_3^2 \sin(\phi_3 - \phi_2)$$
$$= ad \sin(\phi_2 + \theta_1^*), \quad (52)$$

$$\ddot{\phi}_2 \cos(\phi_3 - \phi_2) + e\ddot{\phi}_3 + \dot{\phi}_2^2 \sin(\phi_3 - \phi_2)$$
$$= d \sin(\phi_3 + \theta_1^*). \quad (53)$$

Integrating (51) gives

$$a\dot{\phi}_2 \cos \phi_2 + \dot{\phi}_3 \cos \phi_3 = \frac{(\tau_1^* + \beta_1 \sin \theta_1^*)t}{\alpha_{13}} + \lambda_1, \quad (54)$$

where λ_1 is a constant. Since $E = E^*$ is bounded, the left-hand side term of (54) is bounded for all t. Thus,

$$\tau_1^* = -\beta_1 \sin \theta_1^*; \quad (55)$$

otherwise, the right-hand side term of (54) is infinite as $t \to \infty$. Integrating (54) yields

$$a \sin \phi_2 + \sin \phi_3 = \lambda_1 t + \lambda. \quad (56)$$

Since the left-hand side term of (56) is bounded for all t, $\lambda_1 = 0$ must hold; otherwise, the right-hand side term of (56) is infinite as $t \to \infty$. Thus, (42) and (43) hold.

If $\sin \theta_1^* = 0$, summing (52) and (53) and using (56) with $\lambda_1 = 0$ yields

$$\frac{\mathrm{d}}{\mathrm{d}t}(b\dot{\phi}_2 + e\dot{\phi}_3 + (\dot{\phi}_2 + \dot{\phi}_3)\cos(\phi_2 - \phi_3)) = \pm d\lambda, \quad (57)$$

where "+" and "−" correspond to $\theta_1^* = 0$ and $\theta_1^* = \pi$ (mod 2π), respectively. Integrating (57) with respect to time t gives

$$b\dot{\phi}_2 + e\dot{\phi}_3 + (\dot{\phi}_2 + \dot{\phi}_3)\cos(\phi_2 - \phi_3) = \pm d\lambda t + \lambda_2, \quad (58)$$

where λ_2 is a constant. Since the left-hand-side term of (58) is bounded due to the boundedness of E^*, we obtain $\lambda = 0$; otherwise, the right-hand side term of (58) is infinite as $t \to \infty$.

To obtain the polynomial in (40) in terms of $\sin \phi_2$, in the following derivation, we eliminate $\sin \phi_3$ by using $\sin \phi_3 = \lambda - a \sin \phi_2$ due to (43), and we eliminate $\cos^i \phi_2$ or $\cos^i \phi_3$ with $i \geq 2$ if exists via using

$$\cos^2 \phi_2 = 1 - \sin^2 \phi_2, \text{ or}$$
$$\cos^2 \phi_3 = 1 - \sin^2 \phi_3 = 1 - (\lambda - a\sin\phi_2)^2, \quad (59)$$

which guarantees the highest order of $\cos \phi_2$ or $\cos \phi_3$ if exists equal to one.

Regarding Step 1.2, using (51)–(53) with (55) gives

$$\begin{bmatrix} a\cos\phi_2 & \cos\phi_3 & \sigma_{11} \\ b & \cos(\phi_3 - \phi_2) & \sigma_{12} \\ \cos(\phi_3 - \phi_2) & e & \sigma_{13} \end{bmatrix} \begin{bmatrix} \ddot{\phi}_2 \\ \ddot{\phi}_3 \\ 1 \end{bmatrix} = \begin{bmatrix} 0 \\ 0 \\ 0 \end{bmatrix}, \quad (60)$$

where

$$\sigma_{11} = -a\dot{\phi}_2^2 \sin\phi_2 - \dot{\phi}_3^2 \sin\phi_3,$$
$$\sigma_{12} = -\dot{\phi}_3^2 \sin(\phi_3 - \phi_2) - ad\sin(\phi_2 + \theta_1^*),$$
$$\sigma_{13} = \dot{\phi}_2^2 \sin(\phi_3 - \phi_2) - d\sin(\phi_3 + \theta_1^*).$$

Thus, the determinant of the 3×3 matrix in (60) is 0; otherwise, $\begin{bmatrix} \ddot{\phi}_2, \ddot{\phi}_3, 1 \end{bmatrix} = \begin{bmatrix} 0, 0, 0 \end{bmatrix}$ which raises a contradiction. By computing the determinant and using (59), we obtain (44), where

$$F_1 = d\Bigg(\sin\left(\theta_1^*\right)\Big(-2a + b + a^2 e + 2a\lambda^2 - b\lambda^2$$
$$-2a\lambda\left(2a - b + \cos(\phi_2)\cos(\phi_3)\right)$$
$$\times \sin(\phi_2) + a\left(2 + 2a^2 - a(b + e) - 2\lambda^2\right.$$
$$+ 2a\cos(\phi_2)\cos(\phi_3)\Big)\sin^2(\phi_2)$$
$$+ 4a^2\lambda\sin^3(\phi_2) - 2a^3\sin^4(\phi_2)\Big) + \cos\left(\theta_1^*\right)$$
$$\times \Big(a(-1 + ae)\cos(\phi_2)\sin(\phi_2)$$
$$+ (a - b)\cos(\phi_3)\left(-\lambda + a\sin(\phi_2)\right)\Big)\Bigg),$$

$$F_2 = -(a - b)\cos(\phi_2)\cos(\phi_3)\left(-\lambda + a\sin(\phi_2)\right)$$
$$+ \sin(\phi_2)\Big(a\lambda^2 - b\left(-1 + ae + \lambda^2\right)$$
$$+ 2a(-a + b)\lambda\sin(\phi_2) + a^2(a - b)\sin^2(\phi_2)\Big),$$

$$F_3 = (a - b)e\lambda + (a(-a + b)e + (1 - ae)\cos$$
$$\times (\phi_2)\cos(\phi_3))\sin(\phi_2)$$
$$+ \lambda(1 - ae)\sin^2(\phi_2) + a(-1 + ae)\sin^3(\phi_2).$$

Writing out $E = E^*$ with (9), $\theta_1 \equiv \theta_1^*$, (34), (39) and (43), we obtain (45) directly.

Regarding Step 1.3, first, we eliminate $\dot{\phi}_3$. To this end, by computing $((44) \times e/2 - (45) \times F_3) \times \cos\phi_3$ and using (42) to eliminate $\dot{\phi}_3 \cos\phi_3$, we obtain

$$G_{11} + G_{12}\dot{\phi}_2^2 = 0, \quad (61)$$

where G_{1i} ($i = 1, 2$) are the following functions of $\sin\phi_2$, $\cos\phi_2$, and $\cos\phi_3$:

$$G_{11} = \frac{1}{2}\Bigg(-2\cos(\phi_2)\sin(\phi_2)\Big(-1 + \lambda^2$$
$$-2a\lambda\sin(\phi_2) + a^2\sin^2(\phi_2)\Big)$$
$$\times \left(\gamma - ae\gamma + ade\sin\left(\theta_1^*\right)\left(-\lambda + a\sin(\phi_2)\right)\right)$$
$$+ d\cos\left(\theta_1^*\right)\Big(\left(-1 + \lambda^2 - 2a\lambda\sin(\phi_2) + a^2\sin^2(\phi_2)\right)$$
$$\times \left(3(a - b)e\lambda + a(2 - 5ae + 3be)\sin(\phi_2)\right.$$
$$-2(-1 + ae)\lambda\sin^2(\phi_2)$$
$$+ 4a(-1 + ae)\sin^3(\phi_2)\Big) + \cos(\phi_2)\cos$$
$$(\phi_3)\Big(2a(-a + b)e\lambda$$
$$+ \left(2a^3 e + a^2 e(-2b + e) + 2\left(-1 + \lambda^2\right)\right.$$
$$+ a\left(e - 2e\lambda^2\right)\Big)\sin(\phi_2)$$
$$+ 6a(-1 + ae)\lambda\sin^2(\phi_2) - 4a^2(-1 + ae)\sin^3(\phi_2)\Big)\Bigg)$$

$$+ \cos(\phi_3)\Big(-2\gamma\,(\lambda - a\sin(\phi_2))\,((-a+b)e$$

$$+(-1+ae)\sin^2(\phi_2)\Big)$$

$$+ de\sin(\theta_1^*)\Big(b + a^2 e - b\lambda^2 + 2a\left(-1+\lambda^2\right)$$

$$+ 2a(-2a+b)\lambda\sin(\phi_2)$$

$$+ a\left(2 + 2a^2 - a(b+e) - 2\lambda^2\right)\sin^2(\phi_2)$$

$$+ 4a^2\lambda\sin^3(\phi_2) - 2a^3\sin^4(\phi_2)\Big)\Big)\Big), \quad (62)$$

$$G_{12} = \frac{1}{2}\Big(\cos(\phi_3)\Big(\left(2a^2 - 3ab + b^2\right)e\lambda$$

$$- e\left(2a^3 - 3a^2 b + a\left(b^2 + be - \lambda^2\right)\right.$$

$$+ b\left(-1+\lambda^2\right)\Big)\sin(\phi_2)$$

$$+ \left(-b - 8a^2 e + a(4 + 5be)\right)\lambda\sin^2(\phi_2)$$

$$+ a\left(b + 7a^2 e - 4a(1 + be)\right)\sin^3(\phi_2)$$

$$+ 4a(-1+ae)\lambda\sin^4(\phi_2)$$

$$- 4a^2(-1+ae)\sin^5(\phi_2)\Big)$$

$$+ \cos(\phi_2)\Big(-(a-b)e\lambda\left(-1+\lambda^2\right)$$

$$+ \left(b\left(-1+\lambda^2\right) + a^2 e\left(-3+7\lambda^2\right)\right.$$

$$- 2a\left(-1+\lambda^2 + be\left(-1+3\lambda^2\right)\right)\Big)$$

$$\times \sin(\phi_2)$$

$$+ a\left(-2b - 11a^2 e + a(4 + 9be)\right)\lambda\sin^2(\phi_2)$$

$$+ a\left(-2 + 5a^3 e - 2a^2(1 + 2be) + 4\lambda^2\right.$$

$$+ a\left(b + 2e - 4e\lambda^2\right)\Big)\sin^3(\phi_2)$$

$$+ 8a^2(-1+ae)\lambda\sin^4(\phi_2) - 4a^3(-1+ae)\sin^5(\phi_2)\Big)\Big). \quad (63)$$

Next, multiplying $\cos^2\phi_3$ to (45) and using (42) to eliminate $\dot{\phi}_3\cos\phi_3$ to obtain

$$G_{21} + G_{22}\dot{\phi}_2^2 = 0, \quad (64)$$

where G_{2i} $(i = 1, 2)$ are the following functions of $\sin\phi_2$, $\cos\phi_2$, and $\cos\phi_3$:

$$G_{21} = \left(\gamma - d\cos(\theta_1^*)\left(a\cos(\phi_2) + \cos(\phi_3)\right)\right)$$

$$\times \left(-1 + \lambda^2 - 2a\lambda\sin(\phi_2) + a^2\sin^2(\phi_2)\right), \quad (65)$$

$$G_{22} = \frac{1}{2}\Big(b + a^2 e - b\lambda^2 + 2a\left(-1+\lambda^2\right)$$

$$- 2a\lambda\left(2a - b + \cos(\phi_2)\cos(\phi_3)\right)$$

$$\times \sin(\phi_2) + a\left(2 + 2a^2 - a(b+e)\right.$$

$$- 2\lambda^2 + 2a\cos(\phi_2)\cos(\phi_3)\Big)\sin^2(\phi_2)$$

$$+ 4a^2\lambda\sin^3(\phi_2) - 2a^3\sin^4(\phi_2)\Big). \quad (66)$$

Eliminating $\dot{\phi}_2^2$ from (61) and (64) yields

$$G_{11}G_{22} - G_{12}G_{21} = 0. \quad (67)$$

By using (59), we can guarantee that the highest order of $\cos\phi_3$ of the left-hand side term of the above equation is less than or equal to one. Thus, (67) can be expressed by (47), where

$$Q_1 = Q_{11} + Q_{12}\cos\theta_1^*, \quad (68)$$
$$Q_2 = Q_{21} + Q_{22}\cos\theta_1^*, \quad (69)$$

where Q_{ij} $(i, j = 1, 2)$ are the following functions of $\sin\phi_2$ and $\cos\phi_2$:

$$Q_{11} = 2\cos(\phi_2)\left(-1 + \lambda^2 - 2a\lambda\sin(\phi_2) + a^2\sin^2(\phi_2)\right)$$

$$\left((a-b)\gamma\lambda\left(-1+\lambda^2\right)\right.$$

$$+ a\left(\gamma\left(a\left(ae - 3\lambda^2\right) + b\left(-1 + 3\lambda^2\right)\right)\right.$$

$$+ 2d\lambda\left(b + a^2 e - b\lambda^2\right.$$

$$+ 2a\left(-1+\lambda^2\right)\right)\sin(\theta_1^*)\Big)\sin(\phi_2) + a^2\left(3(a-b)\gamma\lambda\right.$$

$$- 2d\left(b + a^2 e - 3b\lambda^2 + a\left(-2 + 6\lambda^2\right)\right)\sin(\theta_1^*)\Big)\sin^2(\phi_2)$$

$$+ a^2\left(\left(1 - a^2 + a(b-e)\right)\gamma\right.$$

$$- 2d\lambda\left(-2 - 6a^2 + 3ab + ae + 2\lambda^2\right)\sin(\theta_1^*)\Big)$$

$$\times \sin^3(\phi_2) + 2a^3 d\left(-2 - 2a^2 + a(b+e) + 6\lambda^2\right)\sin(\theta_1^*)$$

$$\sin^4(\phi_2) - 12a^4 d\lambda\sin(\theta_1^*)\sin^5(\phi_2)$$

$$+ 4a^5 d\sin(\theta_1^*)\sin^6(\phi_2)\Big), \quad (70)$$

$$Q_{12} = -d\left(-1 + \lambda^2 - 2a\lambda\sin(\phi_2) + a^2\sin^2(\phi_2)\right)$$

$$\left(-(a-b)\lambda\left(b + 3a^2 e - b\lambda^2\right)\right.$$

$$+ \left(5a^4 e - a^3(2 + 3be) - 2b\left(-1+\lambda^2\right)^2\right.$$

$$+ a^2\left(b - 3b\lambda^2\right)$$

$$+ a\left(-2be\left(-1+\lambda^2\right) + 2\lambda^2\left(-1+\lambda^2\right)\right.$$

$$+ b^2\left(-1 + 3\lambda^2\right)\right)\Big)\sin(\phi_2)$$

$$+ a\lambda\left(3a^2(b+e) + a\left(4 - 3b^2 + be - 8\lambda^2\right)\right.$$

$$+ 8b\left(-1+\lambda^2\right)\Big)\sin^2(\phi_2)$$

$$+ a^2 \Big(-a^2(b + 7e) + 4b\left(1 - 3\lambda^2\right) + a\left(2 + b^2\right.$$
$$+ be + 12\lambda^2\Big)\Big) \sin^3(\phi_2)$$
$$+ 8a^3(-a + b)\lambda \sin^4(\phi_2) + 2a^3$$
$$\left(-1 + a^2 + a(-b + e)\right) \sin^5(\phi_2)\Big), \qquad (71)$$

$$Q_{21} = -2\gamma\Big(a^2(-a + b)e\lambda - \left(-a\left(a^3 e - \lambda^2 + \lambda^4\right)\right.$$
$$+ b\left(a^3 e + ae\left(-1 + \lambda^2\right)\right.$$
$$+ \left(-1 + \lambda^2\right)^2\Big)\Big)\sin(\phi_2)$$
$$+ a\lambda\left(2a^2 e + a\left(1 + be - 4\lambda^2\right) + 4b\left(-1 + \lambda^2\right)\right)$$
$$\times \sin^2(\phi_2) + 2a^2\left(b - 3b\lambda^2 + a\left(-ae + 3\lambda^2\right)\right)\sin^3(\phi_2)$$
$$+ a^2\left(1 - 4a^2 + 4ab - ae\right)\lambda\sin^4(\phi_2)$$
$$+ a^3\left(-1 + a^2 + a(-b + e)\right)$$
$$\times \sin^5(\phi_2)\Big) + d\sin\left(\theta_1^*\right)$$
$$\left(\left(b + a^2 e - b\lambda^2 + 2a\left(-1 + \lambda^2\right)\right)^2\right.$$
$$- 4a(2a - b)\lambda\left(b + a^2 e - b\lambda^2 + 2a\left(-1 + \lambda^2\right)\right)\sin(\phi_2)$$
$$+ 2a\left(2a^4 e - a^3\left(4 + be + e^2 - 12\lambda^2\right) + 2b\left(-1 + \lambda^2\right)^2\right.$$
$$- 4a^2\left(e\left(-1 + \lambda^2\right) + b\left(-1 + 3\lambda^2\right)\right)$$
$$+ a\left(-4 + 10\lambda^2 - 6\lambda^4 + be\left(-1 + \lambda^2\right) + b^2\right.$$
$$\left(-1 + 3\lambda^2\right)\Big)\Big)\sin^2(\phi_2)$$
$$- 4a^2\lambda\left(4a^3 - 4a^2(b + e) + a\left(10 + b^2 + be - 12\lambda^2\right)\right.$$
$$+ 4b\left(-1 + \lambda^2\right)\Big)$$
$$\times \sin^3(\phi_2) + a^2\left(4 + 4a^4 - 4a^3(b + 2e) - 12\lambda^2 + 8\lambda^4\right.$$
$$+ a^2\left(20 + b^2 + 2be + e^2 - 72\lambda^2\right) + 4a\left(e\left(-1 + \lambda^2\right)\right.$$
$$+ b\left(-2 + 6\lambda^2\right)\Big)\Big)$$
$$\times \sin^4(\phi_2) + 8a^3\lambda\left(3 + 6a^2 - a(2b + e) - 4\lambda^2\right)\sin^5(\phi_2)$$
$$+ 4a^4\left(-3 - 3a^2 + a(b + e) + 12\lambda^2\right)\sin^6(\phi_2)$$
$$- 32a^5\lambda\sin^7(\phi_2) + 8a^6\sin^8(\phi_2)\Big), \qquad (72)$$

$$Q_{22} = d\cos(\phi_2)\left(-2(a - b)\lambda\left(a^3 e + \left(-1 + \lambda^2\right)^2\right)\right.$$
$$+ a\left(-a^2 e + a^3 e(-2b + e)\right.$$
$$+ 2a^4 e - a\left(2 + 3be - 10\lambda^2\right)\left(-1 + \lambda^2\right)$$
$$- 5b\left(1 - 3\lambda^2 + 2\lambda^4\right)\Big)\sin(\phi_2)$$

$$+ 2a^2\lambda\Big(2a^2 e + a$$
$$\left(5 + 2be - 10\lambda^2\right) + b\left(-9 + 10\lambda^2\right)\Big)\sin^2(\phi_2)$$
$$- a^3\left(-7b - e + 4a^2 e + 20b\lambda^2\right.$$
$$+ a\left(2 + be + e^2 - 20\lambda^2\right)\Big)\sin^3(\phi_2)$$
$$- 2a^3\left(-1 + 5a^2 + a(-5b + e)\right)\lambda\sin^4(\phi_2)$$
$$+ 2a^4\left(-1 + a^2 + a(-b + e)\right)\sin^5(\phi_2)\Big). \qquad (73)$$

Regarding Step 1.4, from (47), we obtain $Q_1^2 - Q_2^2\cos^2\phi_3 = Q_1^2 - Q_2^2(1 - \sin^2\phi_3) = 0$, which can be expressed as (48) by using (59), where the expressions of R_1 and R_2 are omitted for brevity. If $\cos\theta_1^* = 0$, we can show that R_2, the coefficient of $\cos\phi_2$ of $Q_1^2 - Q_2^2\cos^2\phi_3$, is 0. Indeed, from (68) and (70), we obtain $Q_1 = Q_{11} = \cos(\phi_2)\widehat{Q}_{11}$ with $\widehat{Q}_{11}$ not containing $\cos\phi_2$; from (69) and (72), we know that $Q_2 = Q_{21}$ does not contain $\cos(\phi_2)$. Thus, $Q_1^2 - Q_2^2(1 - \sin^2\phi_3) = Q_{11}^2 - Q_{21}^2(1 - \sin^2\phi_3) = (1 - \sin^2\phi_2)\widehat{Q}_{11}^2 - Q_{21}^2(1 - \sin^2\phi_3)$ does not contain $\cos\phi_2$. Hence, this shows that if $\cos\theta_1^* = 0$, then $R_2 = 0$.

Details of Step 2

Regarding Step 2, we prove that (41) does not hold by showing that there exists $0 < i \le N$ such that $\xi_i \ne 0$ for any mechanical parameters $a, b, d,$ and e defined by (34), and parameters $\theta_1^*, \lambda,$ and γ. To start, regarding (50), from

$$\xi_{28} = 256a^{20}d^4(a^2 - ab - ae + 1)^4\sin^2\theta_1^* \qquad (74)$$

and $\xi_{28} = 0$, we need to consider whether

$$a^2 - ab - ae + 1 \ne 0; \qquad (75)$$

that is, $e \ne (1 + a^2 - ab)/a$, and we analyze Cases 1 and 2 below:

Case 1: $e \ne (1 + a^2 - ab)/a$

From (74) and $\xi_{28} = 0$, we have $\sin\theta_1^* = 0$. This yields

$$\xi_{24} = 16a^{16}d^4(a^2 - ab + ae - 1)^2$$
$$(a^2 - ab - ae + 1)^4 > 0, \qquad (76)$$

which contradicts (41). Indeed, $a^2 - ab + ae - 1 > 0$ due to $a \geq b > 0$ and $ae > 1$ from Lemma 6.

Case 2: $e = (1 + a^2 - ab)/a$

From Lemma 7, we have $a \neq 1$ and $a > b$. In this case, we obtain

$$\xi_{24} = 256a^{18}(a - b)^2 d^2 \lambda^2 \sin^2(\theta_1^*)\epsilon, \tag{77}$$

where

$$\begin{aligned}\epsilon =&(1 - 7a^2 + 6ab)^2 d^2 \lambda^2 \cos^2 \theta_1^* \\ &+ ((1 - 3a^2 + 2ab)\gamma - 4a(a - b)d\lambda \sin \theta_1^*)^2. \end{aligned} \tag{78}$$

From (77) and $\xi_{24} = 0$, we consider two cases of $\lambda = 0$ and $\lambda \neq 0$, separately.

Case 2.1: $e = (1 + a^2 - ab)/a$ and $\lambda = 0$

We obtain

$$\xi_0 = (-1 + a^2)^8(a - b)^8 d^4 \sin^4 \theta_1^*. \tag{79}$$

Since $a \neq 1$ and $a > b$ from Lemma 7, we see that $\xi_0 = 0$ shows $\sin \theta_1^* = 0$. This yields

$$\xi_{18} = 16a^{14}(-1+a^2)^2(a-b)^4(1+3a^2-4ab)^2 d^2 \gamma^2. \tag{80}$$

Regarding whether $1 + 3a^2 - 4ab \neq 0$ holds or not, we consider Cases 2.1.1 and 2.1.2 below:

Case 2.1.1: $e = (1 + a^2 - ab)/a$, $\lambda = 0$, and $b \neq (1 + 3a^2)/(4a)$

From (80) and $\xi_{18} = 0$, we obtain $\gamma = 0$. This yields

$$\xi_{16} = 9a^{12}(-1+a^2)^4(a-b)^4(1+3a^2-4ab)^2 d^4 > 0, \tag{81}$$

which contradicts (41).

Case 2.1.2: $e = (1 + a^2 - ab)/a$, $\lambda = 0$, and $b = (1 + 3a^2)/(4a)$

We have

$$\xi_{12} = \frac{a^4(-1+a^2)^{10}(1+a^2)^2 d^4}{1024} > 0, \tag{82}$$

which contradicts (41).

Case 2.2: $e = (1 + a^2 - ab)/a$ and $\lambda \neq 0$

We show $\sin \theta_1^* \neq 0$. On the contrary, assume $\sin \theta_1^* = 0$, from Step 1.1, we have $\lambda = 0$ which raises a contradiction. Thus, from (77) and $\xi_{24} = 0$, we have $\epsilon = 0$ yielding $1 - 3a^2 + 2ab \neq 0$ due to (78); otherwise, if $1 - 3a^2 + 2ab = 0$, then $\epsilon \geq (4a(a - b)d\lambda \sin \theta_1^*)^2 > 0$. Thus, $\epsilon = 0$ shows

$$(1 - 7a^2 + 6ab) \cos \theta_1^* = 0, \tag{83}$$

$$\gamma = \frac{4a(a - b)d\lambda \sin \theta_1^*}{1 - 3a^2 + 2ab}. \tag{84}$$

We treat $\cos \theta_1^* \neq 0$ and $\cos \theta_1^* = 0$, separately.

Case 2.2.1: $e = (1+a^2-ab)/a$, $\lambda \neq 0$, and $\cos \theta_1^* \neq 0$

From (83), we obtain $b = (7a^2 - 1)/(6a)$. This together with (84) gives

$$\xi_{22} = \frac{16}{9} a^{14}(-1 + a^2)^2 d^4 \lambda^2 \sin^2(\theta_1^*)\rho, \tag{85}$$

where

$$\begin{aligned}\rho =& 9((-1 + a^2)^2 - 2(1 + a^2)\lambda^2)^2 \cos^2 \theta_1^* \\ &+(5(-1 + a^2)^2 - 6(1 + a^2)\lambda^2)^2 \sin^2 \theta_1^* \geq 0. \end{aligned}$$

From (85) and $\xi_{22} = 0$, we have $\rho = 0$ which yields $(-1 + a^2)^2 - 2(1 + a^2)\lambda^2 = 0$ and $5(-1 + a^2)^2 - 6(1+a^2)\lambda^2 = 0$. Deleting λ^2 from these two equalities yields $-1 + a^2 = 0$ which contradicts $a \neq 1$ in (38).

Case 2.2.2: $e = (1+a^2-ab)/a$, $\lambda \neq 0$, and $\cos \theta_1^* = 0$

From Step 1.4, using $\cos \theta_1^* = 0$ shows $R_2 = 0$, below we study $L = R_1 = 0$ in (49) rather than $L = R_1^2 = 0$ in (50). Though the highest order of R_1 in (49) is 14, when $e = (1 + a^2 - ab)/a$ and (84) hold, we find that $\xi_{14} = \xi_{13} = \xi_{12} = 0$ holds, and

$$\xi_{11} = \frac{16a^8(a-b)d^2\lambda\left(12a(1+a^2)(a-b)\lambda^2 - (-1+a^2)^2(1+3a^2-4ab)\right)}{-1+3a^2-2ab}. \tag{86}$$

Using $\xi_{11} = 0$, $a > b$, and $\lambda \neq 0$, we obtain

$$\lambda^2 = \frac{(-1 + a^2)^2(1 + 3a^2 - 4ab)}{12a(1 + a^2)(a - b)}. \tag{87}$$

Using (87), we have

$$\xi_i = k_i \widehat{\xi}_i, \quad i = 10, 9, 8, \tag{88}$$

where k_i are nonzero terms due to $a \neq 1$ and $\lambda \neq 0$, and

$$\begin{aligned}\widehat{\xi}_{10} =& 6 - 14a^2 - 23a^4 - 14a^6 + 21a^8 \\ &+ a(23 + a^2 + 31a^4 - 7a^6)b \\ &- 8a^2(1 + a^2 + a^4)b^2, \end{aligned} \tag{89}$$

$$\begin{aligned}\widehat{\xi}_9 =& 11 - 2a^2 - 125a^4 - 97a^6 + 138a^8 + 315a^{10} \\ &+ a(8 + 196a^2 + 94a^4 + 80a^6 - 570a^8)b \\ &+ 2a^2(-89 + 17a^2 - 163a^4 + 67a^6)b^2 \\ &+ 96a^3(1 + a^2 + a^4)b^3, \end{aligned} \tag{90}$$

$$\begin{aligned}\widehat{\xi}_8 =& 35 - 209a^2 - 240a^4 + 1420a^6 + 2159a^8 \\ &- 933a^{10} - 3042a^{12} + 2538a^{14} \end{aligned}$$

$$+ (185a - a^3(266 + 2211a^2 + 1808a^4$$
$$+ 3193a^6 - 7050a^8 + 4941a^{10}))b$$
$$+ 2a^2(-11 + 1091a^2 - 678a^4 + 2714a^6$$
$$- 1439a^8 + 915a^{10})b^2$$
$$+ 96a^3(3 - 10a^2 - 6a^4 - 9a^6 + 4a^8)b^3. \quad (91)$$

Thus, $\xi_i = 0$ $(i = 10, 9, 8)$ are equivalent to

$$\widehat{\xi}_i = 0, \quad i = 10, 9, 8. \quad (92)$$

Below we show that there do not exist $a \neq 1$ and b satisfying (92). To this end, first, we use $\widehat{\xi}_{10} = 0$ and $\widehat{\xi}_9 = 0$ to delete b to obtain the following polynomial equation:

$$\delta_1 = 3703 - 7609z + 3744z^2 - 7609z^3 + 3703z^4 = 0,$$
$$\text{with } z = a^2 > 0. \quad (93)$$

Indeed, to derive δ_1 in (93), since the highest order of b in (89) is 2, we divide $\widehat{\xi}_9$ by $\widehat{\xi}_{10}$ with respect to b to obtain $\widehat{\xi}_9 = p_9\widehat{\xi}_{10} + r_9$, where p_9 is the quotient and r_9 is the remainder with the highest order of b being equal to 1. Using $r_9 = \widehat{k}_9\widehat{r}_9$, where $\widehat{k}_9 \neq 0$ due to $a \neq 1$, and

$$\widehat{r}_9 = -338 + 512a^2 + 1437a^4 + 2795a^6 + 1945a^8$$
$$+ 1785a^{10} - a(1447 + 1010a^2$$
$$+ 3222a^4 + 1010a^6 + 1447a^8)b. \quad (94)$$

From $\widehat{\xi}_{10} = 0$ and $\widehat{\xi}_9 = 0$, we have $r_9 = 0$ and $\widehat{r}_9 = 0$. Moreover, we divide $\widehat{\xi}_{10}$ by $\widehat{r}_9$ with respect to b to obtain $\widehat{\xi}_{10} = p_{10}\widehat{r}_9 + r_{10}$ with p_{10} being the quotient and r_{10} being the remainder. From $\widehat{\xi}_{10} = 0$ and $\widehat{r}_9 = 0$, we have $r_{10} = 0$. Using $r_{10} = \psi_{10}\delta_1$ with $\psi_{10} \neq 0$ due to $a \neq 1$ yields $\delta_1 = 0$ in (93).

Next, we use $\widehat{\xi}_{10} = 0$, $\widehat{\xi}_8 = 0$, and $\widehat{r}_9 = 0$ to delete b to obtain the following polynomial equation:

$$\delta_2 = 244 + 355z - 1726z^2 + 355z^3 + 244z^4 = 0,$$
$$\text{with } z = a^2 > 0. \quad (95)$$

To derive δ_2 in (95), we divide $\widehat{\xi}_8$ by $\widehat{\xi}_{10}$ with respect to b to obtain $\widehat{\xi}_8 = p_8\widehat{\xi}_{10} + r_8$ with p_8 being the quotient and r_8 being the remainder with the highest order of b being equal to 1. Using $r_8 = \widehat{k}_8\widehat{r}_8$, where $\widehat{k}_8 \neq 0$ due to $a \neq 1$ and

$$\widehat{r}_8 = 2558 - 5332a^2 - 12433a^4 - 9329a^6$$
$$+ 13432a^8 + 29542a^{10}$$

$$+ 36075a^{12} + 25839a^{14} + \Big(10873a$$
$$+ 1174a^3 + 3937a^5 - a^7$$
$$\times \big(19216 + 35113a^2 + 21046a^4 + 20961a^6\big)\Big)b.$$
$$(96)$$

From $\widehat{\xi}_{10} = 0$ and $\widehat{\xi}_8 = 0$, we have $r_8 = 0$ and $\widehat{r}_8 = 0$. Finally, we divide $\widehat{r}_8$ by $\widehat{r}_9$ with respect to b to obtain $\widehat{r}_8 = \widehat{p}_8\widehat{r}_9 + d_8$ with $\widehat{p}_8$ being the quotient and d_8 being the remainder. Thus, from $\widehat{r}_8 = 0$ and $\widehat{r}_9 = 0$, we obtain $d_8 = 0$. Using $d_8 = \psi_8\delta_2$ with $\psi_8 \neq 0$ due to $a \neq 1$ yields $\delta_2 = 0$ in (95).

Since $z = a^2 > 0$ and the positive real solutions of (93) and (95) are

$$z = 0.5148, \quad z = 1.9425, \quad (97)$$
$$z = 0.5486, \quad z = 1.8228, \quad (98)$$

respectively, (93) and (95) do not have a common positive solution; thus, they do not hold simultaneously. This contradicts (92), equivalently, (88), and thus contradicts (41).

For Cases 1 and 2, we have shown that (41) does not hold for any mechanical parameters a, b, d, and e defined by (34), and any possible parameters θ_1^*, λ, and γ. Thus, $\dot{\theta}_2 = \dot{\phi}_2 \equiv 0$. From (42), we have $\dot{\phi}_3 \cos\phi_3 = 0$. Integrating it with respect to time yields $\sin\phi_3 = \lambda_0$ with λ_0 being a constant. Thus, ϕ_3 is a constant and $\dot{\theta}_3 = \dot{\phi}_3 \equiv 0$. This completes the proof of Lemma 3. □

Appendix 4: Proof of Lemma 4

We characterize the invariant set W in (20) by studying $E^* = E_r$ and $E^* \neq E_r$, separately. To start, putting $E(\boldsymbol{\theta}(t), \dot{\boldsymbol{\theta}}(t)) \equiv E^*$ and $\theta_1(t) \equiv \theta_1^*$ into (32) (from which we derived controller (15)) yields

$$(E^* - E_r)\tau_1(t) + k_P\theta_1^* \equiv 0. \quad (99)$$

If $E^* = E_r$, then $\theta_1^* = 0$ from (99). Putting $\theta_1^* = 0$ into the W in (20), we obtain the W_r in (24). Putting $\dot{\theta}_2(t) = 0$ and $\dot{\theta}_3(t) = 0$ into the W_r in (24) to obtain equilibrium points in the W_r in (24), we obtain $\cos\theta_2(t) = 1$ and $\cos\theta_3(t) = 1$. This shows that $\theta_2(t) = 0$ and $\theta_3(t) = 0$ (mod 2π). Thus, the UEP is the only equilibrium point in W_r.

If $E^* \neq E_r$, then $\tau_1(t)$ is a constant from (99), denoted as τ_1^*. From Lemma 3, links 2 and 3 do not

move. Thus, the APP robot stays at an equilibrium an equilibrium configuration $\boldsymbol{\theta}^* = \begin{bmatrix} \theta_1^*, \theta_2^*, \theta_3^* \end{bmatrix}^{\mathrm{T}}$. Below we show that if k_P satisfies (22), then the APP robot stays at an equilibrium point belongs to Ω_s in (25). Using (4) and (32) (from which we derived controller (15)) with equilibrium torque $\tau_1^* = -\beta_1 \sin \theta_1^*$ and the energy at the point $E^* = P(\boldsymbol{\theta}^*)$, we have

$$\sin \theta_2^* \equiv 0, \quad \sin \theta_3^* \equiv 0, \tag{100}$$

$$\beta_1(E_r - P(\boldsymbol{\theta}^*)) \sin \theta_1^* + k_P \theta_1^* = 0. \tag{101}$$

Note that (100) gives

$$\theta_i^* = 0 \text{ or } \pi \pmod{2\pi}, \quad i = 2, 3. \tag{102}$$

Clearly, $\theta_1^* = 0$ is a solution of (101). When $\theta_1^* \neq 0$, we rewrite (101) as

$$k_P = f_0(\theta_1^*), \tag{103}$$

where

$$f_0(\theta_1^*) = \frac{-\beta_1(E_r - P(\boldsymbol{\theta}^*)) \sin \theta_1^*}{\theta_1^*}, \quad \theta_1^* \neq 0. \tag{104}$$

Since $f_0(\theta_1^*)$ is an even function of θ_1^*, we can see that (103) has no solution θ_1^* if and only if

$$k_P > \max_{\theta_1^* > 0} f_0(\theta_1^*). \tag{105}$$

Since the numerator of $f_0(\theta_1^*)$ is a periodic function with period 2π and is nonnegative in $[\pi, \; 2\pi]$, we have

$$\max_{\theta_1^* > 0} f_0(\theta_1^*) = \max_{\pi \le \theta_1^* \le 2\pi} f_0(\theta_1^*). \tag{106}$$

For all θ_2^* and θ_3^* in (102), since $P(\boldsymbol{\theta}^*) \ge \beta_1 \cos \theta_1^* - \beta_2 - \beta_3$, we can see that (103) has no solution if and only if k_P satisfies (22).

Thus, under controller (15) with the bounds on the gains in (17), (18), and (22), the closed-loop solution $(\boldsymbol{\theta}(t), \dot{\boldsymbol{\theta}}(t))$ converges to either the W_r in (24) when $E^* = E_r$ or the Ω_s in (25) when $E^* \neq E_r$. □

Appendix 5: Proof of Lemma 5

The proof of the four equilibrium points being strictly unstable is similar to that in [30]. First, let J_{uuu} be the Jacobian matrix evaluated at the UEP $(\theta_1, \theta_2, \theta_3, \dot{\theta}_1, \dot{\theta}_2, \dot{\theta}_3) = (0, 0, 0, 0, 0, 0)$. Straightforward calculation of the characteristic polynomial of that point yields

$$|sI - J_{uuu}| = s^6 + a_1 s^5 + a_2 s^4 + a_3 s^3 \\ + a_4 s^2 + a_5 s + a_6,$$

where

$$a_1 = \frac{k_V}{k_D},$$

$$a_2 = \frac{k_P}{k_D} - \frac{\alpha_{33}\beta_2 + \alpha_{22}\beta_3}{\alpha_{22}\alpha_{33} - \alpha_{23}^2},$$

$$a_3 = -\frac{k_V(\alpha_{33}\beta_2 + \alpha_{22}\beta_3)}{k_D(\alpha_{22}\alpha_{33} - \alpha_{23}^2)},$$

$$a_4 = \frac{-k_P(\alpha_{23}\beta_2 + \alpha_{22}\beta_3) + k_D\beta_2\beta_3}{k_D(\alpha_{22}\alpha_{33} - \alpha_{23}^2)},$$

$$a_5 = \frac{k_V\beta_2\beta_3}{k_D(\alpha_{22}\alpha_{33} - \alpha_{23}^2)},$$

$$a_6 = \frac{k_P\beta_2\beta_3}{k_D(\alpha_{22}\alpha_{33} - \alpha_{23}^2)}.$$

Since $\alpha_{22}\alpha_{33} - \alpha_{23}^2 > 0$ which can be verified directly by using (8), $a_3 < 0$ holds for all mechanical parameters of the APP robot in (8) and control gains $k_D > 0$, $k_P > 0$, and $k_V > 0$. Therefore, J_{uuu} has at least one eigenvalue in the open right-half plane. This shows that the UEP is strictly unstable.

Second, let J_{uud} be the Jacobian matrix evaluated at the up–up–down equilibrium point $(\theta_1, \theta_2, \theta_3, \dot{\theta}_1, \dot{\theta}_2, \dot{\theta}_3) = (0, 0, \pi, 0, 0, 0)$. Straightforward calculation of the characteristic polynomial of that point yields

$$|sI - J_{uud}| = s^6 + a_1 s^5 + a_2 s^4 + a_3 s^3 \\ + a_4 s^2 + a_5 s + a_6,$$

where

$$a_1 \Delta = (\alpha_{22}\alpha_{33} - \alpha_{23}^2)k_V,$$

$$a_2 \Delta = (\alpha_{22}\alpha_{33} - \alpha_{23}^2)k_P + (-\alpha_{33}\beta_2 + \alpha_{22}\beta_3)k_D \\ + 2\beta_3((\alpha_{22}\alpha_{33} - \alpha_{23}^2)\beta_1 + (\alpha_{11}\alpha_{33} - \alpha_{13}^2)\beta_2 \\ - (\alpha_{11}\alpha_{22} - \alpha_{12}^2)\beta_3),$$

$$a_3 \Delta = (-\alpha_{33}\beta_2 + \alpha_{22}\beta_3)k_V,$$

$$a_4 \Delta = 2\beta_3(\alpha_{11}\beta_1\beta_2 + \alpha_{22}\beta_1\beta_3 - \alpha_{33}\beta_1\beta_2) \\ + (-\alpha_{33}\beta_2 + \alpha_{22}\beta_3)k_P - \beta_2\beta_3 k_D,$$

$$a_5 \Delta = -\beta_2\beta_3 k_V,$$

$$a_6 \Delta = -\beta_2\beta_3(k_P + 2\beta_1\beta_3),$$

with $\Delta = (\alpha_{22}\alpha_{33} - \alpha_{23}^2)k_D + 2(\alpha_{12}^2\alpha_{33} + \alpha_{22}\alpha_{13}^2 - 2\alpha_{12}\alpha_{13}\alpha_{23} - \alpha_{11}(\alpha_{22}\alpha_{33} - \alpha_{23}^2))\beta_3$.

Below we show $\Delta > 0$. From condition (17), we have $k_D > k_{uud}$, where

$$k_{uud} = (E_r - P(\boldsymbol{\theta}))\,(\boldsymbol{b}^{\mathrm{T}} \boldsymbol{M}^{-1}(\boldsymbol{\theta})\boldsymbol{b})^{-1}|_{\theta_1=0,\,\theta_2=0,\,\theta_3=\pi}$$
$$= \frac{\rho_1}{\alpha_{22}\alpha_{33} - \alpha_{23}^2},$$

with $\rho_1 = 2\beta_3(\alpha_{11}\alpha_{22}\alpha_{33} - \alpha_{12}^2\alpha_{33} - \alpha_{22}\alpha_{13}^2 + 2\alpha_{12}\alpha_{13}\alpha_{23} - \alpha_{11}\alpha_{23}^2)$. Thus, we have $\Delta = (k_D - k_{uud})(\alpha_{22}\alpha_{33} - \alpha_{23}^2) > 0$. This shows that $a_5 < 0$ and $a_6 < 0$ for all mechanical parameters of the APP robot in (8) and control gains $k_D > 0$, $k_P > 0$, and $k_V > 0$. Therefore, J_{uud} has at least one eigenvalue in the open right-half plane. This shows that the up–up–down equilibrium point is strictly unstable. Similarly, we can show that the up–down–up equilibrium point $(\theta_1, \theta_2, \theta_3, \dot{\theta}_1, \dot{\theta}_2, \dot{\theta}_3) = (0, \pi, 0, 0, 0, 0)$ is also strictly unstable; the detail is omitted for brevity.

Finally, regarding the up–down–down equilibrium point $(\theta_1, \theta_2, \theta_3, \dot{\theta}_1, \dot{\theta}_2, \dot{\theta}_3) = (0, \pi, \pi, 0, 0, 0)$, different from the other two equilibrium points in Ω_s, we cannot show its instability from the signs of coefficients of the characteristic polynomial of that point, and we need to compute the Hurwitz determinants (see, e.g., [16]). Let J_{udd} be the Jacobian matrix evaluated at that point. Straightforward calculation of the characteristic polynomial of that point yields

$$|sI - J_{udd}| = s^6 + a_1 s^5 + a_2 s^4 + a_3 s^3 + a_4 s^2 + a_5 s + a_6,$$

where

$$a_1 \Xi = (\alpha_{22}\alpha_{33} - \alpha_{23}^2)k_V,$$
$$a_2 \Xi = (\alpha_{22}\alpha_{33} - \alpha_{23}^2)k_P + (\alpha_{33}\beta_2 + \alpha_{22}\beta_3)k_D$$
$$\quad + 2(\beta_2 + \beta_3)$$
$$\quad \times \big((\alpha_{22}\alpha_{33} - \alpha_{23}^2)\beta_1 - (\alpha_{11}\alpha_{33} - \alpha_{13}^2)\beta_2$$
$$\quad - (\alpha_{11}\alpha_{22} - \alpha_{12}^2)\beta_3\big),$$
$$a_3 \Xi = (\alpha_{33}\beta_2 + \alpha_{22}\beta_3)k_V,$$
$$a_4 \Xi = (\alpha_{33}\beta_2 + \alpha_{22}\beta_3)k_P + \beta_2\beta_3 k_D$$
$$\quad - 2(\alpha_{11}\beta_2\beta_3 - \alpha_{22}\beta_1\beta_3 - \alpha_{33}\beta_1\beta_2)(\beta_2 + \beta_3),$$
$$a_5 \Xi = \beta_2\beta_3 k_V,$$
$$a_6 \Xi = \beta_2\beta_3(k_P + 2\beta_1(\beta_2 + \beta_3)),$$

with $\Xi = (\alpha_{22}\alpha_{33} - \alpha_{23}^2)k_D - 2(\alpha_{11}\alpha_{22}\alpha_{33} - \alpha_{12}^2\alpha_{33} - \alpha_{22}\alpha_{13}^2 + 2\alpha_{12}\alpha_{13}\alpha_{23} - \alpha_{11}\alpha_{23}^2)(\beta_2 + \beta_3)$.

Similar to $\Delta > 0$, we can show $\Xi > 0$. In fact, from condition (17), we have $k_D > k_{udd}$, where

$$k_{udd} = (E_r - P(\boldsymbol{\theta}))\,(\boldsymbol{b}^{\mathrm{T}} \boldsymbol{M}^{-1}(\boldsymbol{\theta})\boldsymbol{b})^{-1}|_{\theta_1=0,\,\theta_2=\pi,\,\theta_3=\pi}$$
$$= \frac{\rho_2}{\alpha_{22}\alpha_{33} - \alpha_{23}^2},$$

where $\rho_2 = 2(\beta_2 + \beta_3)(\alpha_{11}\alpha_{22}\alpha_{33} - \alpha_{12}^2\alpha_{33} - \alpha_{22}\alpha_{13}^2 + 2\alpha_{12}\alpha_{13}\alpha_{23} - \alpha_{11}\alpha_{23}^2)$. Thus, $\Xi = (k_D - k_{udd})(\alpha_{22}\alpha_{33} - \alpha_{23}^2) > 0$. Using $\Xi > 0$ shows $a_1 > 0$, $a_3 > 0$, $a_5 > 0$, and $a_6 > 0$ for any mechanical parameters described in (8) for the APP robot, and control gains $k_D > 0$, $k_P > 0$, and $k_V > 0$. However, the sign of a_2 or a_4 depends on the mechanical and control gains. We obtain the Hurwitz determinant

$$D_3 = \begin{vmatrix} a_1 & a_3 & a_5 \\ 1 & a_2 & a_4 \\ 0 & a_1 & a_3 \end{vmatrix} = a_1 a_2 a_3 - a_3^2 - a_1^2 a_4 + a_1 a_5,$$

which satisfies

$$D_3 \Xi^3$$
$$= -2k_V^2(\beta_2 + \beta_3)\Big(2\alpha_{23}\beta_2\beta_3(\alpha_{12}\alpha_{23} - \alpha_{22}\alpha_{13})$$
$$(\alpha_{12}\alpha_{33} - \alpha_{13}\alpha_{23}) + \alpha_{33}\beta_2^2(\alpha_{12}\alpha_{33} - \alpha_{13}\alpha_{23})^2$$
$$+ \alpha_{22}\beta_3^2(\alpha_{22}\alpha_{13} - \alpha_{12}\alpha_{23})^2\Big).$$

Using Lemma 6 shows $\alpha_{12}\alpha_{23} - \alpha_{22}\alpha_{13} \geq 0$ and $\alpha_{12}\alpha_{33} - \alpha_{13}\alpha_{23} > 0$. Thus, $D_3 < 0$. Therefore, J_{udd} has at least one eigenvalue in the open right-half plane. This shows that the up–down–down equilibrium point is strictly unstable. □

References

1. Acosta, J., Ortega, R., Astolfi, A., Mahindrakar, A.: Interconnection and damping assignment passivity-based control of mechanical systems with underactuation degree one. IEEE Trans. Autom. Control **50**(12), 1936–1955 (2005)
2. Aguilar-Ibañez, C., Mendoza-Mendoza, J.A., Martinez, J.C., Jesus Rubio, J., Suarez-Castanon, M.S.: A limit set stabilization by means of the Port Hamiltonian system approach. Int. J. Robust Nonlinear Control **25**(12), 1739–1750 (2015)
3. Almutairi, N.B., Zribi, M.: On the sliding mode control of a ball on a beam system. Nonlinear Dyn. **59**(1–2), 221–238 (2010)
4. Asano, F., Luo, Z.W.: Dynamic analyses of underactuated virtual passive dynamic walking. In: Proceedings of 2007 IEEE International Conference on Robotics and Automation, pp. 3210–3217. IEEE (2007)

5. Bowden, C., Holderbaum, W., Becerra, V.M.: Strong structural controllability and the multilink inverted pendulum. IEEE Trans. Autom. Control **57**(11), 2891–2896 (2012)

6. Cefalo, M., Lanari, L., Oriolo, G.: Energy-based control of the butterfly robot. In: Proceedings of the 3rd IFAC workshop on Periodic Control Systems (2006)

7. Chemori, A., Marchand, N.: A prediction-based nonlinear controller for stabilization of a non-minimum phase PVTOL aircraft. Int. J. Robust Nonlinear Control **18**(8), 876–889 (2008)

8. Colgate, J.E., Lynch, K.M.: Mechanics and control of swimming: a review. IEEE J. Ocean. Eng. **29**(3), 660–673 (2004)

9. Fang, Y., Ma, B., Wang, P., Zhang, X.: A motion planning-based adaptive control method for an underactuated crane system. IEEE Trans. Control Syst. Technol. **20**(1), 241–248 (2012)

10. Fantoni, I., Lozano, R.: Non-linear Control for Underactuated Mechanical Systems. Springer, Berlin (2001)

11. Fantoni, I., Lozano, R., Spong, M.W.: Energy based control of the Pendubot. IEEE Trans. Autom. Control **45**(4), 725–729 (2000)

12. Grizzle, J.W., Moog, C.H., Chevallereau, C.: Nonlinear control of mechanical systems with an unactuated cyclic variable. IEEE Trans. Autom. Control **50**(5), 559–575 (2005)

13. Jiang, Z.P.: Global tracking control of underactuated ships by Lyapunov's direct method. Automatica **38**(2), 301–309 (2002)

14. Khalil, H.K.: Nonlinear Systems, 3rd edn. Prentice-Hall, New Jersey (2002)

15. Kolesnichenko, O., Shiriaev, A.S.: Partial stabilization of underactuated Euler–Lagrange systems via a class of feedback transformations. Systems & Control Letters **45**(2), 121–132 (2002)

16. Kuo, B.C.: Automatic Control Systems, 6th edn. Prentice Hall, New Jersey (2001)

17. Liu, Y., Xin, X.: Set-point control for folded configuration of 3-link underactuated gymnastic planar robot: new results beyond the swing-up control. Multibody Syst. Dyn. **34**(4), 349–372 (2015)

18. Ma, X., Su, C.Y.: A new fuzzy approach for swing up control of Pendubot. In: Proceedings of the 2002 American Control Conference, pp. 1001–1006 (2002)

19. Martinez, R., Alvarez, J.: A controller for 2-DOF underactuated mechanical systems with discontinuous friction. Nonlinear Dyn. **53**(3), 191–200 (2008)

20. Nishimura, H., Funaki, K.: Motion control of three-link brachiation robot by using final-state control with error learning. IEEE/ASME Trans. Mechatron. **3**(2), 120–128 (1998)

21. Ortega, R., Spong, M.W., Gomez-Estern, F., Blankenstein, G.: Stabilization of a class of underactuated mechanical systems via interconnection and damping assignment. IEEE Trans. Autom. Control **47**(8), 1218–1233 (2002)

22. Qian, C., Lin, W.: A continuous feedback approach to global strong stabilization of nonlinear systems. IEEE Trans. Autom. Control **46**(7), 1061–1079 (2001)

23. Rentia, N., Vira, N.: Why symbolic computation in robotics? Comput. Ind. **17**(1), 49–62 (1991)

24. Seifried, R.: Integrated mechanical and control design of underactuated multibody systems. Nonlinear Dyn. **67**(2), 1539–1557 (2012)

25. Shiriaev, A.S., Fradkov, A.L.: Stabilization of invariant sets for nonlinear non-affine systems. Automatica **36**(11), 1709–1715 (2000)

26. Spong, M.W.: The swing up control problem for the Acrobot. IEEE Control Syst. Mag. **15**(1), 49–55 (1995)

27. Sun, N., Fang, Y., Chen, H.: Adaptive antiswing control for cranes in the presence of rail length constraints and uncertainties. Nonlinear Dyn. **81**(1), 41–51 (2015)

28. Sun, N., Fang, Y., Zhang, X.: An increased coupling-based control method for underactuated crane systems: theoretical design and experimental implementation. Nonlinear Dyn. **70**(2), 1135–1146 (2012)

29. Udwadia, F.E., Koganti, P.B.: Dynamics and control of a multi-body planar pendulum. Nonlinear Dyn. **81**(1), 845–866 (2015)

30. Xin, X.: Analysis of the energy-based swing-up control for the double pendulum on a cart. Int. J. Robust Nonlinear Control **21**(4), 387–403 (2011)

31. Xin, X.: On simultaneous control of the energy and actuated variables of underactuated mechanical systems-example of the Acrobot with counterweight. Adv. Robot. **27**(12), 959–969 (2013)

32. Xin, X., Kaneda, M.: Analysis of the energy based swing-up control of the Acrobot. Int. J. Robust Nonlinear Control **17**(16), 1503–1524 (2007)